1968

Limit analysis and limit equilibrium solutions in soil mechanics, June 1968 (70-19)

W. F. Chen

C. Scawthorn

Soil Mechanics and Theories of Plasticity

LIMIT ANALYSIS AND LIMIT EQUILIBRIUM SOLUTIONS IN SOIL MECHANICS

by
Wai F. Chen
Charles R. Scawthorn

Fritz Engineering Laboratory Report No. 355.3

Soil Mechanics and Theories of Plasticity

LIMIT ANALYSIS AND LIMIT EQUILIBRIUM SOLUTIONS IN SOIL MECHANICS

by

Wai F. Chen
Charles R. Scawthorn

Fritz Engineering Laboratory
Department of Civil Engineering
Lehigh University
Bethlehem, Pennsylvania

June 1968

Fritz Engineering Laboratory Report No. 355.3

TABLE OF CONTENTS

ABSTRACT

Idealizations in soil mechanics are usually necessary in order to obtain solutions and to have these solutions in a readily applicable form. Limit equilibrium has been a method of solving various soil stability problems.

One weakness of the limit equilibrium method has been the neglect of the stress-strain relationship of the soil. According to the mechanics of solids, this condition must be satisfied for a complete solution. Limit analysis, through the concept of a yield criterion and its associated flow rule, considers the stress-strain relationship. However, a soil with cohesion and internal friction is not modeled accurately by a theory of perfect plasticity. Nevertheless, indications are that the stability problems in soil mechanics will, in time, be computed on the basis of the limit theorems of plasticity. A discussion is given, therefore, of the significance of the limit analysis in terms of the real behavior of soils and their idealizations. With this background, the meaning of existing limit equilibrium solutions is discussed, and the power and simplicity of application of the limit analysis method is demonstrated.

1. INTRODUCTION

Soil mechanics, a science of relatively recent origin, has been well developed since Karl Terzaghi's[1] pioneering efforts in the early twentieth century. As pointed out by Drucker[2], one peculiar feature of soil mechanics has been the lack of interrelation between methods used to treat similar problems with different purposes in mind.

In foundation problems, for instance, the stress distribution under a footing is determined from Boussinesq's solution for the stress distribution under a vertical load on a semi-infinite plane--a solution from linear elasticity theory. On the other hand, the bearing capacity of a footing is determined using limit equilibrium (or the slipline solution) of plasticity theory. The calculation of the settlement of a footing actually utilizes visco-elastic theory to describe the material behavior with time.

The reasons for treating the problems differently are evident: The key to obtaining the complete solution, starting with a consideration of elastic action and proceeding to contained plastic flow, and finally unrestricted plastic flow, requires the basic knowledge of the stress-strain relations for soils in the elastic as well as the inelastic range. No such general relations have been determined as yet, for an inelastic soil. Even with an appropriate idealized stress-strain relationship, the details of the distribution of stress and strain in the complete solution are far too complicated and probably not possible. The solutions, if

possible to obtain, would be too involved and impractical for application. Necessary idealizations and simplifications are, therefore, used by engineers to obtain solutions for practical problems. These simplified analyses must, ultimately, be justified by comparison with available rigorous solutions, or, in the event these are lacking, experimental results.

As an illustration of this point, let us examine a problem and the simplifications involved. In order to solve stability problems, which are the primary concern of this paper, such as lateral earth pressures, bearing capacity, or stability of vertical cuts, use is made of only limit equilibrium conditions[3] (that is, the stress conditions in ideal soils immediately preceeding ultimate failure). No thought is given to the corresponding state of strain. This method of attack raises doubts, if one recalls from mechanics of solids, that a valid solution requires satisfying the boundary conditions, equations of equilibrium (or of motion), equations of compatibility, and the stress-strain relationship. It is this stress-strain relationship which connects equilibrium to compatibility, and which distinguishes elasticity from plasticity or visco-elasticity theories. Without considering the stress-strain relationship, a so-called solution is merely a guess. On the other hand, the limit equilibrium approach simplifies the theoretical analysis drastically, and provides good predictions of the ultimate load of soil stability problems which are otherwise unavailable for practical applications.

A more rigorous approach is to consider the stress-strain relationship in an idealized manner. This idealization, termed normality (or the flow rule)[4], establishes the limit theorems[5] on which limit analysis is based. Within the framework of this assumption, the approach is rigorous and the techniques are competitive with those of limit equilibrium, in some instances being much simpler. The plastic limit theorems of Drucker, Prager, and Greenberg[5] may conveniently be employed to obtain upper and lower bounds of the ultimate load for stability problems, such as the critical heights of unsupported vertical cuts, or the bearing capacity of nonhomogeneous soils.

It is the objective of this paper, through a review of the standard and widely known techniques used in the solutions of soil stability problems, to accomplish two purposes. The first is to discuss the meaning and nature of existing, "classical", soil mechanics solutions from the limit analysis point of view. Many of the techniques will be shown to implicitly contain the basic philosophy of one or both of the plastic limit theorems.

The second purpose is to demonstrate the usefulness and power of the plastic limit theorems in developing a limit analysis technique. Useful information, although sometimes crude, will be quickly obtained. It will be seen, by comparing numerical results of the classical and limit analysis solutions, that good agreement is usually obtained. The limit analysis technique will provide new solutions, or an alternative method which is more rational than existing techniques.

This discussion will be restricted to perfectly plastic soils that are assumed to conform to the Coulomb Yield Criterion and its associated flow rule. Three types of typical stability problems will be examined:

(1) The critical height of a vertically unsupported cut,

(2) Active and passive lateral earth pressure, and

(3) The bearing capacity of soils.

2. FUNDAMENTALS OF LIMIT ANALYSIS

2.1 Basic Concepts

The mechanical behavior of soils is usually described as having both cohesion, c, and internal friction, ϕ. The resistance of soils to deformation is furnished by cohesion and friction across the possible slip planes in a mass of material. The generally accepted law of failure in soil mechanics is Coulomb's criterion[1], which states that slip occurs when, on any plane at any point in a mass of soil, the shear stress, τ ($>o$) reaches an amount that depends linearly upon the cohesion and the normal stress, σ (here taken to be positive in compression), i.e. (Fig. 1)

$$\tau = c + \sigma \tan\phi \qquad (1)$$

For illustrative purposes, a simple physical model, shown in Fig. 2, may be helpful. In the figure, a layer of dense granular material is subjected to the action of two forces. The force P_n acts at right angles to the plane 1-1, whereas the other, the force P_t, acts tangentially to that plane. Let us further assume that P_n remains constant during the experiment, whereas, P_t gradually increases from zero to the value which will produce sliding. At the instant of sliding, the value P_t must not only overcome cohesion, but also must exceed the resistance furnished by two types of friction. The first of these arises on the contact surfaces of adjoining particles and is termed surface friction. The second, offered by the interference of the particles

themselves to changes of their relative position, is termed interlocking friction. It is this interlocking friction that requires the displacement upward, as well as the usual displacement to the side. The displacement vector must, therefore, make an angle θ to the slip plane.

If soil were idealized as perfectly plastic with Coulomb's law of yielding, then Eq. (1) defines the yield curve in the stress space σ, τ. If now a stress state, represented by a vector from the origin, is increased from zero, yield will be incipient when the vector reaches the curve (two straight lines). For a perfectly plastic material, the vector representing the stress state at any given point can never protrude beyond the curve, since it is an unattainable stress state in granular media.

Let us further assume that the stress-strain relation is such that the plastic strain rate vector is always normal to the yield curve when their corresponding axes are superimposed (Fig. 1). It can be seen from the figure that this is equivalent to assuming $\theta=\phi$ in Fig. 2. The perfectly-plastic idealization with associated flow rule (normality) is illustrated by a block shearing on a horizontal plane, Fig. 3a. Volume expansion is seen to be a necessary accompaniment to shearing deformation according to the idealizations. This theory was proposed by Drucker and Prager[6] and generalized later by Drucker[7], and Shield[8].

In contrast to the above mentioned effort, one may idealize soil as a frictional material for which the interlocking friction is ignored. Deformation occurs by the smooth sliding of adjacent surfaces of material points (See Fig. 3b). If $\tan\phi$ in expression (1) denotes the coefficient of friction between adjacent surfaces of material points along the plane, expression (1) becomes the well-known Coulomb friction limit condition for the shear strength of soil. The important difference between Coulomb friction and perfectly-plastic Coulomb action is seen in Fig. 3, where frictional sliding is horizontal while perfectly-plastic shearing involves large upward vertical motion. If the plastic strain rate vector is superimposed to the Coulomb limit curves (assumed as yield curve), the normality rule does not hold (See Fig. 1). The extent of this endeavor is described in a recent work by Dais[9].

Real soils are quite complex and are still imperfectly understood. They are neither truly frictional in behavior, nor are they plastic. Hence, any such idealized treatment, as discussed above, will either result in some differences between predictions and experimental facts, or will entertain certain mathematical difficulties. For example, the dilatation which is predicted by perfect plastic theory to accompany the shearing action will usually be larger than that found in practice[10]. The inadequacy of a perfectly plastic idealization has been discussed by Drucker[2,11,12] and DeJong[13] among others. The lack of uniqueness for solutions to problems using friction theory has been exhibited and explored by Dais[9].

In order to improve upon the perfectly plastic theory, Drucker, Gibson, and Henkel introduced the strain-hardening theories of soil plasticity[14], which were later extended by Jenike and Shield[15]. The work-hardening plastic action may involve upward or downward vertical motion, or neither, of the sliding block as illustrated in Fig. 3, which qualitatively agrees with experimental data. Recently, more sophisticated theories have been proposed by Weidler and Paslay[16], Spencer[17], and Sobotka[18,19] on non-homogeneous soils in an attempt to overcome some of the known deficiencies in previous theories. Clearly the development of a more sophisticated theory will almost always bring a more elaborate stress-strain relation. Solutions to practically important problems, on the contrary, become exceedingly difficult to obtain, if the stress-strain relation is too involved. A compromise must, therefore, be made between convenience and physical reality.

In certain circumstances, such as in the stability problems of soil mechanics, there appears to be reasonable justification for the adoption of a limit analysis approach based upon Coulomb's yield criterion and its associated flow rule in soils, as discussed in Section 1.

2.2 Limit Theorems

The foundations of limit analysis are the two limit theorems[5]. For any body or assemblage of bodies of elastic-perfectly plastic material they may be stated, in terminology appropriate to

soil mechanics, as:

Theorem 1 (lower bound)--If an equilibrium distribution of stress can be found which balances the applied load and nowhere violates the yield criterion, which includes c, the cohesion, and $\emptyset$, the angle of internal friction, the soil mass will not fail, or will be just at the point of failure.

Theorem 2 (upper bound)--The soil mass will collapse if there is any compatible pattern of plastic deformation for which the rate of work of the external loads exceeds the part of internal dissipation.

According to the statement of the theorems, in order to properly bound the "true" solution, it is necessary to find a compatible failure mechanism (velocity field or flow pattern) in order to obtain an upper bound solution. A stress field satisfying all conditions of Theorem 1 will be required for a lower bound solution. If the upper and lower bounds provided by the velocity field and stress field coincide, the exact value of the collapse, or limit, load is determined.

2.3 The Dissipation Functions

As stated in the upper bound theorem, it is necessary to compare the rate of internal dissipation of energy with the rate of work of external forces. The dissipation of energy, D, per unit volume due to a plastic strain rate is, therefore, of primary importance. It can

be shown in general that the dissipation function has the simpler form[20]

$$D = 2\ c\ \tan\left(\frac{\pi}{4} - \frac{\phi}{2}\right) \Sigma\ \dot{\epsilon}_t \qquad (2)$$

where $\dot{\epsilon}_t$ denotes a positive principal component of the plastic strain rate tensor.

For the particular case of plane strain, the expression (2) reduces to

$$D = c\ \cos\phi\ \dot{\gamma}_{max} \qquad (3)$$

where $\dot{\gamma}_{max} = [(\dot{\epsilon}_x - \dot{\epsilon}_y)^2 + \dot{\gamma}_{xy}^2]^{1/2}$ is the maximum rate of engineering shear strain.

An alternative derivation in terms more familiar to the engineer will be discussed in what follows. The discussion will be restricted to the plane strain case. A number of familiar shear deformation zones, which are especially useful for soil mechanics, are treated as illustrative examples. The results are adequate in connection with later application. Some of the results have been discussed by Chen[21].

Homogeneous Shearing Zone--The energy dissipated in the homogeneous shearing zone, Fig. 4, is

$$P_t (t\dot{\gamma}) - P_n (t\dot{\gamma}\tan\phi) \tag{4}$$

in which $\dot{\gamma}$ is the shear strain rate and t is the thickness of the zone. The dimension perpendicular to the plane of the paper in Fig. 4 is taken as unity and the width of the zone is denoted by b. Then the rate of energy dissipated per unit volume, D, is the total dissipation in Eq. (4) divided by the volume, bt:

$$D = \dot{\gamma} \left(\frac{P_t}{b} - \frac{P_n}{b} \tan\phi \right)$$

or

$$D = \dot{\gamma} (\tau - \sigma \tan\phi) \tag{5}$$

Since the Coulomb yield criterion must be satisfied in the plastic zone it follows from Eq. (1) that

$$D = c\,\dot{\gamma} \tag{6}$$

It should be noted that the shear strain rate, $\dot{\gamma}$, in the zone is not the maximum shear strain rate $\dot{\gamma}_{max}$, but is related by $\dot{\gamma} = \dot{\gamma}_{max} \cos\phi$. This is the consequence of volume expansion accompanied by plastic shearing. The Mohr circle shown in the figure indicates clearly the relationship between $\dot{\gamma}$ and $\dot{\gamma}_{max}$.

Figure 5 shows a number of examples of differently shaped homogeneous shearing zones. Fig. 5a is a part of Fig. 4 as shown by

the dotted lines in the figure. Fig. 5b is the half field of homogeneous deformation of Fig. 5a, while a proper rigid body rotation of Fig. 5b results in the interesting field of Fig. 5c.

Narrow transition layer--If the thickness t in Fig. 4 is very thin, the homogeneous shearing zone may be imagined, as in Fig. 6, to be a simple discontinuity with a discontinuous tangential velocity $\delta u = t\dot{\gamma}$ and a discontinuous normal separation $\delta v = t\dot{\gamma} \tan \phi = \delta u \tan\phi$. The rate of dissipation of work per unit of discontinuity surface is

$$D_A = \frac{P_t}{b} \delta u - \frac{P_n}{b} \delta v$$

or (7)

$$D_A = \delta u (\tau - \sigma \tan\phi) = c\delta u$$

Figure 6 shows clearly that a simple slip δu must always be accompanied by a separation δv for $\phi \neq 0$. The familiar circular surface of discontinuity is, therefore, not a permissible surface for rigid body sliding because of the separation requirement for c-ϕ soils. The plane surface and the logarithmic spiral surface of angle ϕ are the only two surfaces of discontinuity which permit rigid body motions relative to a fixed surface.

Zone of radial shear when τ=c--An approximation to a zone of radial shear is given in Fig. 7a where six rigid triangles at an equal

central angle $\Delta\theta$ are shown. Energy dissipation takes place along the radial lines O-A, O-B, O-C, etc. due to the discontinuity in velocity between the triangles. Energy is also dissipated on the discontinuous surface D-A-B-C-E-F-G since the material below this surface is considered at rest. Since the material must remain in contact with the surface D-A-B-C-E-F-G, the triangles must move parallel to the arc surfaces. The rigid triangles must also remain in contact with each other. Hence, the compatible velocity diagram of Fig. 7b shows that each triangle of the mechanism must have the same speed.

With expression (7), the rate of dissipation of energy can easily be calculated. The energy dissipation along the radial line O-B, for example, is the cohesion c multiplied by the relative velocity, δu, and the length of the line of discontinuity, r:

$$c\ r\ (2V \sin \frac{\Delta\theta}{2}) \tag{8}$$

where the relative velocity δu, appears as $(2V \sin \frac{\Delta\theta}{2})$. Similarly, the energy dissipation along the discontinuous surface A-B is

$$c\ (2r \sin \frac{\Delta\theta}{2})\ V \tag{9}$$

where the length of A-B is $(2r \sin \frac{\Delta\theta}{2})$ and $\delta u = V$. Since the energy dissipation along the radial line O-B is the same as along the arc surface A-B, it is natural to expect that the total energy dissipation

in the zone of radial shear, D-O-G, with a central angle Θ will be identical with the energy dissipated along the arc D-G. This is evident since Fig. 7a becomes closer and closer to the zone of radial shear as the number n increases. At the limit, when n approaches infinity, the zone of radial shear is recovered. The total energy dissipated in the zone of radial shear is the sum of the energy dissipated along each radial line when the number n approaches infinity:

$$D = \lim_{n \to \infty} \left(2\, c\, r\, V \sin \frac{\Theta}{2n}\right) n$$

or

$$D = 2c\, r\, V \lim_{n \to \infty} n \sin \frac{\Theta}{2n}$$

or

$$D = c\, V\, (r\Theta) \tag{10}$$

where

$$\Delta\theta = \frac{\Theta}{n}$$

Log spiral zone of c-ϕ soils--The extension of the above discussion to the more general case of a log spiral zone of c-ϕ soils is evident. A picture of six rigid triangles, at an equal angle $\Delta\theta$ to each other, is shown in Fig. 8a. It is found that the energy dissipation in a log spiral zone of c-ϕ soil is equal to the energy dissipated along the spiral discontinuity surface, which is:

$$D = c \int r\, V\, d\theta = c \int_o^{\Theta} (r_o \exp\theta\tan\phi)\ (V_o \exp\theta\tan\phi)\ d\theta$$

or

$$D = \frac{1}{2}\, c\, V_o\, r_o\, \cot\phi\ (\exp 2\Theta \tan\phi - 1) \qquad (11)$$

where V_o, r_o, and Θ are shown in Fig. 8a. A detailed discussion of the log spiral zone is given in the Appendix.

3. THE STABILITY OF VERTICAL CUTS

3.1 Limit Equilibrium Analysis

The comparison between limit equilibrium and plastic limit analysis can be illustrated by evaluating the stability of soil in a vertical bank. The height at which an unsupported vertical cut, as illustrated in Fig. 9, will collapse due to the weight of the soil will be defined as the critical height, H_{cr}. The conventional analysis (limit equilibrium) will be examined first and then compared to the method of limit analysis.

It is common practice to evaluate this problem by the equilibrium method. The failure surface is assumed to be a plane inclined at an angle θ to the horizontal (See Fig. 9) and Coulomb's law of failure is applied. From Eq. (1),

$$\tau = c + \sigma \tan\phi$$

The distribution of σ and τ along the failure plane is unknown, but if s is the length of the shear plane:

$$\int \tau \, ds = \int c \, ds + \int \sigma \tan\phi \, ds = cs + \tan\phi \int \sigma \, ds \qquad (12)$$

Equilibrium requires that:

$$\int \sigma \, ds = W \cos\theta$$
$$\int \tau \, ds = W \sin\theta \qquad (13)$$

Substituting Eq. (13) into Eq. (12) yields

$$W \sin\theta = c \frac{H_{cr}}{\sin\theta} + W \cos\theta \tan\phi$$

where

$$W = \frac{w H_{cr}^2}{2 \tan\theta} \tag{14}$$

W defines the unit weight of the soil, w, multiplied by the volume of the soil mass above the shear plane. If θ is minimized then:

$$\theta_{cr} = (\frac{1}{4}\pi + \frac{1}{2}\phi) \tag{15}$$

Equation (14) then yields the critical height

$$H_{cr} = \frac{4c}{w} \tan(\frac{1}{4}\pi + \frac{1}{2}\phi) \tag{16}$$

Assuming a curved surface instead of a plane for the sliding surface will reduce the critical height slightly. Fellenius[22] used this condition and found the critical height to be

$$H_{cr} = \frac{3.85c}{w} \tan(\frac{1}{4}\pi + \frac{1}{2}\phi) \tag{17}$$

In this analysis, Coulomb's law is only satisfied along the assumed failure plane. It is not shown, nor known, if Coulomb's law of failure is violated at other points. A valid solution requires that equilibrium,

compatibility (and boundary conditions) and the stress-strain relationship be satisfied. Here only equilibrium has been satisfied. From the limit theorems it is known that this solution is not a lower bound since only equilibrium is satisfied, and not the yield criterion. The solution is merely one of many solutions that satisfy equilibrium. It is not known whether or not it is unique.

3.2 Plastic Limit Analysis

The limit analysis of this problem, first performed by Drucker and Prager[6], involves determining a lower bound on the collapse load by assuming a stress field which satisfies equilibrium and does not violate the yield criterion at any point. An upper bound is obtained by a velocity field compatible with the flow rule in which the rate of work of the external forces equals or exceeds the rate of internal energy dissipation.

Starting first with the upper bound, a mechanism (velocity field) is selected as shown in Fig. 10. As the wedge, formed by the shear plane which makes an angle β with the vertical, slides downward along the discontinuity surface, there is a separation velocity, $V\sin\phi$, from the discontinuity surface. The rate of work done by the external forces is the vertical component of the velocity multiplied by the weight of the soil wedge:

$$\frac{1}{2}wH_{cr}^2 \tan\beta \; V \cos(\phi + \beta) \qquad (18)$$

While the rate of energy dissipated along the discontinuity surface in Eq. (7):

$$c \frac{H_{cr}}{\cos\beta} V \cos\phi \tag{19}$$

Equating the rate of external work to the rate of internal energy dissipation gives:

$$H_{cr} \leq \frac{2c}{w} \frac{\cos\phi}{\sin\beta \cos(\phi+\beta)} \tag{20}$$

If ϕ is minimized then

$$\beta = \frac{1}{4}\pi - \frac{1}{2}\phi \tag{21}$$

and

$$H_{cr} \leq \frac{4c}{w} \tan(\frac{1}{4}\pi + \frac{1}{2}\phi) \tag{22}$$

This is the same value obtained by the method of limit equilibrium. This implies that the limit equilibrium method solution presented previously is an upper bound, unless the solution is exact.

A lower bound can be obtained by constructing a stress field composed of three regions as shown in Fig. 11a. Region I, in the bank itself, is subjected to uniaxial compression, which increases with depth. Region II is under biaxial compression and region III is under hydrostatic pressure ($\sigma_x=\sigma_y$). Fig. 11b shows the corresponding

Mohr circles for each region. Failure occurs when the circle representing Region I meets the yield curve. Therefore,

$$\frac{1}{2}wH = c\cos\phi + \frac{1}{2}wH\sin\phi$$

and (23)

$$H_{cr} \geq \frac{2c}{w}\tan(\frac{1}{4}\pi + \frac{1}{2}\phi)$$

hence, the lower bound solution is only one half the value given by the upper bound solution. If the average is used, $H_{cr} = \frac{3c}{w}\tan(\frac{1}{4}\pi + \frac{1}{2}\phi)$, then the maximum error is 33%.

As indicated by Drucker and Prager[6], the upper bound may be improved by choosing for a discontinuity surface a logarithmic spiral rather than the plane used here (See Fig. 10). The lower bound may be improved by the choice of other stress fields, probably quite complex and which may involve tensile stresses in the soil.

3.3 Soil Unable to Take Tension

In the laboratory soil may exhibit the ability to resist tension. In the field, however, the presence of water, or tensile cracks near the surface, may destroy the tensile strength of the soil. Hence, the tensile strength of soil is not reliable and it may be neglected. This is a conservative idealization. The Coulomb yield criterion is modified by the tension cut-off as shown in Fig. 1 in which the requirement of zero tension is met by the circle termination as

shown (the upper half of the yield curve is 0-D-B).

As the soil is unable to resist tension, the introduction of a tensile crack in a failure mechanism is permissible[6,23,24]. No energy is dissipated in the formation of a simple tension crack; both normal and shear stress are zero on the plane of separation (See the origin in Fig. 1).

The rotational mechanism containing a simple tension crack and a homogeneous shearing zone is shown in Fig. 12. Failure due to tipping over of the soil "slab" of thickness Δ about point A with an angular velocity ω is possible[7]. The region ABC of homogeneous shearing, $\dot{\gamma}$, is the field shown in Fig. 5b which indicates that $\omega = \dot{\gamma}$. Equation (6) then gives $D = c\dot{\gamma} = c\omega$. The total rate of dissipation of internal energy for unit dimension perpendicular to the paper is just D times the area of the triangle ABC or

$$(c\omega)\ [\Delta^2\ \tan(\tfrac{1}{4}\pi + \tfrac{1}{2}\phi)] \qquad (24)$$

The rate of external work, done by gravity, is the weight of the soil moving downward as the "slab" rotates about A, multiplied by the velocity, which is $\omega \frac{\Delta}{2}$

$$W \approx w\ \Delta\ H$$

or (25)

$$\frac{1}{2}\ w\ \Delta^2\ H\ \omega$$

If the rate of external work is equated to the dissipation, and Δ allowed to approach zero, it yields:

$$H_{cr} \leq \frac{2c}{w} \tan(\tfrac{1}{4}\pi + \tfrac{1}{2}\phi) \tag{26}$$

This upper bound, which neglects the tensile stress, agrees with the lower bound for the previous case, where moderate tensile capacity was incorporated into the yield criterion. However, an examination of the stress field for this latter case reveals that no tensile stress exists. Hence, the solution is also a valid for the case of a tension cut-off. Since the upper and lower bound solutions agree, the value of H_{cr} is:

$$H_{cr} = \frac{2c}{w} \tan(\tfrac{1}{4}\pi + \tfrac{1}{2}\phi) \tag{27}$$

This also confirms Terzaghi's[1] solution for a tensile crack extending the full height of the bank.

When comparing the limit analysis approach with the classical limit equilibrium method, the realization that it cannot be regularly or confidently stated that the present limit equilibrium approach is either an upper, or lower, bound is quite important. The limit equilibrium solution does not provide an indication of its own applicability or validity.

The upper bound and lower bound theorems provide a tool which allows one to bound the "true" solution. They provide a guideline for

the inexperienced and the experienced person and the knowledge he requires to properly choose a rational factor of safety. Using limit analysis, the soil mechanician may easily bound a solution. With the error known from this part of his analysis, he may include the error in the material properties, perhaps make allowances for workmanship, and logically calculate a factor of safety. This is the probable course that soil mechanics, with the bounding of solutions, may take. It must be borne in mind that limit analysis is only valid within the framework of the stress-strain relationship (flow rule).

4. LATERAL EARTH PRESSURES

4.1 Introduction

Lateral earth pressure can be divided into active earth pressure and passive earth pressure as illustrated in Fig. 13[25]. It is apparent that the wall may have two directions of motion, into the bank or away from the bank.

If the wall is initially at rest and held by a force $P=P_o$, it is apparent that for a cohesionless soil, as the force P is reduced, the wall will be forced outward due to the weight of the soil. As P is gradually reduced, the soil undergoes first elastic deformation, then elastic-plastic deformation (contained plastic flow, where the elastic and plastic strains are of the same order) and finally, uncontained plastic flow. Figure 13b shows a load-displacement curve depicting the behavior of the soil under active and passive earth pressure. The limiting force $P=P_{an}$ is usually defined as the active earth pressure, which is bounded from below by upper bounds, from above by lower bounds.

The explanation for this lies in the definition of the upper and lower bounds. The lower bound is a load for which the structure will not fail, if equilibrium and the yield criterion are satisfied. The upper bound is a load for which the structure will fail when the rate of external work equals or exceeds the rate of internal energy dissipation in a geometrically admissible velocity field. It is seen in Fig. 13b that the loads for which the wall will not continually displace (fail) lie below the passive earth pressure and above the active

earth pressure. Likewise, the upper bounds lie outside this region, above the passive earth pressure and below the active earth pressure. To approach the true active earth pressure, one must maximize the upper bound and minimize the lower bound.

If the force P is increased from P_o, displacement occurs and failure (continuous displacement under constant load) is the result as the passive earth pressure P_{pn}, is approached. The active and passive definitions are derived from the role the backfill material plays in the two cases. In the active earth pressure case, the failure is due to the soil's weight overcoming the internal friction and pressure on the wall, that is, the soil is playing an active role. In the passive earth pressure case the failure is due to the pressure on the wall overcoming the soil's weight and internal friction, hence, the soil plays a passive role.

First, examine the conventional limit equilibrium approach, introduced by Coulomb[26]. The soil is assumed, in the active earth pressure case, to fail by sliding along a plane inclined at an angle Ω to the vertical, as illustrated in Fig. 14. Since the wedge is in a state of equilibrium, the force polygon indicated in Fig. 14 must close. The force P is the reaction along the back of the wall (the angle of wall firction, δ, is zero); F is the reaction along the face RS, at an angle $\emptyset$ to the normal to RS; and W is the weight of the soil wedge. The wedge angle, Ω, is chosen so that the sliding wedge encounters the least resistance, and the solution is found to be:

$$P_{an} = \frac{1}{2}wH^2 \tan^2(\frac{1}{4}\pi - \frac{1}{2}\phi) \qquad (28)$$

The solution may be generalized to include effects of wall friction, δ; walls inclined at an angle α to the vertical; and backfill inclined at an angle β to the horizontal.

4.2 Plastic Limit Analysis

Next examine the limit analysis solution for a vertical wall with a flat backfill of cohesionless material, as shown in Fig. 15. The active earth pressure corresponds to an outward motion of the wall, caused by the weight of the soil. Therefore, the soil weight is assumed to act as a wedge sliding down and outward, against the wall RT. The mechanism is two rigid bodies with plane sliding surfaces. This is a compatible velocity field for an upper bound solution, since the velocity V of the soil mass RST is at an angle ϕ to the discontinuity surface RS. The rate of external work is in two parts, the rate of work done by the soil weight moving downward and the rate of work done by the force P moving horizontally:

$$(\frac{1}{2}wH^2 \tan\Omega)\ [V \cos(\Omega + \phi)] - PV \sin(\Omega + \phi) \qquad (29)$$

The rate of internal dissipation consists of the energy dissipated along RT and along RS (assume a frictionless wall, which implies no energy dissipated along RT). The total rate of energy dissipation is:

$$cV\cos\phi \tag{30}$$

which, for a cohesionless soil (c=0), is zero. Equating the rate of internal and external work yields:

$$P = \frac{1}{2}wH^2 \tan\Omega \cot(\Omega + \phi) \tag{31}$$

The limit load or the collapse load is obtained by maximizing Ω which yields:

$$\Omega = \frac{1}{4}\pi - \frac{1}{2}\phi$$

and (33)

$$P_{an} = \frac{1}{2}wH^2 \tan^2(\frac{1}{4}\pi - \frac{1}{2}\phi)$$

For the passive earth pressure case, the mechanism is quite similar to the active earth pressure case except that since the motion is upward, the velocity, V, of the soil wedge is reversed, although still directed at an angle ϕ to the discontinuity surface. The rate of internal and external work are found in the same manner as for the active earth pressure, and:

$$\Omega = \frac{1}{4}\pi + \frac{1}{2}\phi \tag{34}$$

and

$$P_{pn} = \frac{1}{2}wH^2 \tan^2(\frac{1}{4}\pi + \frac{1}{2}\phi) \tag{35}$$

The upper bound is then minimized to obtain the passive earth pressure.

To obtain lower bounds, Fig. 16 shows a discontinuous equilibrium solution[27] in which k is a parameter which is chosen such that the Coulomb yield criterion will be satisfied. The Mohr's circles in the figure shows clearly that two extreme values of k are possible which furnish the needed lower bound solutions of the lateral earth pressure problem. From the figure, one obtains:

for active earth pressure

$$k = k_a = \tan^2(\tfrac{1}{4}\pi - \tfrac{1}{2}\phi) \tag{36}$$

for passive earth pressure

$$k = k_p = \tan^2(\tfrac{1}{4}\pi + \tfrac{1}{2}\phi) \tag{37}$$

Equilibrium is then determined

$$P = \int_o^H kwy \, dy \tag{38}$$

The results indicate that the upper and lower bounds for the active earth pressure and the passive earth pressure, respectively, agree, indicating the exact solution.

The case considered is a special case of the general problem, where β is the backfill angle, δ the wall friction angle ($\delta<\phi$), and α

the wall angle as shown in Fig. 17. All may assume different values, as well as $\emptyset$ the angle of internal friction, and c, the cohesion. For $\alpha=90^{\circ}$, the case of a vertical wall, the velocity components are shown in Fig. 18 for the case when the failure mechanism is assumed to be a plane. The failure plane RS is of length:

$$\frac{H \cos\beta}{\cos(\Omega+\beta)} \tag{39}$$

and the wedge is of weight:

$$W = \frac{1}{2}wH^2 \frac{\sin\Omega \cos\beta}{\cos(\Omega+\beta)} \tag{40}$$

The rate of external work is:

for the active case

$$W\ V \cos(\Omega+\emptyset) - P_{an}\ V \sin(\Omega+\emptyset) \tag{41}$$

for the passive case

$$-W\ V \cos(\Omega-\emptyset) + P_{pn}\ V \sin(\Omega-\emptyset) \tag{42}$$

For either case, the rate of energy dissipated internally along RS is:

$$c\ V \cos\emptyset \frac{H \cos\beta}{\cos(\Omega+\beta)} \tag{43}$$

The energy dissipated by sliding friction between the wall and the wedge is:

for the active case

$$P_{an} \tan\delta \; V \cos(\Omega+\phi) \tag{44}$$

for the passive case

$$P_{pn} \tan\delta \; V \cos(\Omega-\phi) \tag{45}$$

where P_{an} and P_{pn} denote the normal to the wall components of the active and passive earth pressures, respectively.

Equating the rate of internal energy dissipation and the rate of external work yields

$$P_{an} = \frac{\cos\beta}{\cos(\Omega+\beta)} \frac{\frac{1}{2}wH^2 \sin\Omega \cos(\Omega+\phi) - cH\cos\phi}{\sin(\Omega+\phi) + \tan\delta \cos(\Omega+\phi)} \tag{46}$$

and

$$P_{pn} = \frac{\cos\beta}{\cos(\Omega+\beta)} \frac{\frac{1}{2}wH^2 \sin\Omega \cos(\Omega-\phi) + cH\cos\phi}{\sin(\Omega-\phi) - \tan\delta \cos(\Omega-\phi)} \tag{47}$$

These equations are valid for a vertical wall, $\delta<\phi$ (otherwise there is shearing of the soil instead of wall friction), and the assumption of a plane for a discontinuity surface. They may be easily rewritten to include α.

The best choice, so as to maximize or minimize P, of the angle of the failure plane, Ω, may not be easily found for the general

solution given by Eqs (46, 47). For special cases, such as discussed above ($c=\delta=\beta=0$), it may be explicitly found or a transcendental equation, which it must satisfy, may be determined. The easiest procedure is to hold constant the values of the different parameters, and increment Ω until the maximum P_{an} or the minimum P_{pn}, is reached. This procedure is suitable for digital computation. Table 1 is a comparison of Coulomb's solution and this upper bound limit analysis solution for a vertical wall with cohesionless material. It may be seen that agreement is good.

In this section, an important soil mechanics problem has been examined from the viewpoint of limit analysis. A solution which agrees with the limit equilibrium solution has been obtained. The derivation was seen to be straightforward. The upper bound in the general case can be improved by considering a rotational discontinuity (logarithmic spiral) instead of the plane translation type. Although no numerical results were presented for a cohesive soil, the general solutions are valid, and may be applied.

5. THE BEARING CAPACITY OF SOILS

In this section certain solutions dealing with the bearing capacity of soils will be evaluated by the methods of limit equilibrium and limit analysis so that a better understanding of the meaning of these solutions will be gained. A brief description of the application of limit analysis to three dimensional soil bearing capacity problems will then be offered so as to demonstrate the power of the method.

5.1 Limit Equilibrium Analysis

First, consider the bearing capacity of a surcharged cohesive soil in which the angle of internal friction, $\emptyset$, is zero. This is illustrated, schematically, in Fig. 19a. It will be assumed that there is no contact between the punch and the surcharge. The limit equilibrium solution takes as its failure mode a rotation of a semi-circular section about its own center, 0, located at the corner of the punch. The distribution of normal stresses along the semi-circular surface is unknown, but the shear stress is assumed to be equal to c, the cohesion. The summation of moments about the center of rotation, 0, is taken:

$$-P\,\frac{b}{2} + \pi b\ c\ b + bhw\,\frac{b}{2} + hc\ b = 0 \qquad (48)$$

where the (hc)b term is due to the shearing of the surcharge material. The resultant of the weight of the rotating soil, as well as the normal stresses along the circumference, pass through the center, 0, and produce no moments. The ultimate bearing capacity of the footing by limit

equilibrium is then[28]:

$$p = \frac{P}{b} = c(2\pi + \frac{2h}{b}) + wh \tag{49}$$

or

$$p = 6.28c(1 + 0.32\,\frac{h}{b} + 0.16\,\frac{wh}{c}) \tag{50}$$

Two other assumptions concerning possible surfaces of failure are given in Fig. 19b,c for purposes of comparison[28]. The first consists in assuming the center of rotation 0 at the edge of the foundation, as shown in Fig. 19b. The choice of this failure mode for a limit equilibrium solution would raise several questions. What is the normal and shear stress distribution along the circular shear plane? Also, what is the normal stress distribution along the vertical separation between the quarter circle and the triangular region? The resultant of the shear stress along this line passes through 0, but the normal stress resultant is not defined. A commonly accepted method in limit equilibrium analysis is to assume the quarter circle rotation produces uni-axial compression of the soil it bears against, as shown in Fig. 19b. The maximum compression that may be sustained by this soil is (2c + wh) since 2c is the greatest allowable difference between principal stresses and wh corresponds to a hydrostatic pressure which is in equilibrium with the surcharge at the top surface. (The pressure due to the weight of the soil within the region is neglected). Summing moments about 0 of all forces, yields:

$$p = \frac{P}{b} = c\ (\pi + 2) + wh = 5.14c + wh \tag{51}$$

for h=0:

$$p = 5.14c \tag{52}$$

which is nearly 20% less than the value of 6.28c obtained in Fig. 19a.

An even lower limit equilibrium solution can be produced by considering the scheme shown in Fig. 19c, which assumes a triangular soil block under the punch. Equilibrium of forces shows that:

$$p = 4c + wh \tag{53}$$

As with other limit equilibrium solutions, it is not known which solutions should be chosen. If it can be shown that the stress field in region I can be extended throughout the soil and still satisfy equilibrium and the yield condition, then this is a lower bound. Unfortunately, it is not known in the present case whether the stress field can be extended in this manner.

5.2 Plastic Limit Analysis--Upper Bounds

To obtain an upper bound of the same problem by limit analysis, the chosen mechanisms as shown in Fig. 20 are quite similar. In Fig. 20a is a rigid body rotation about 0, with shearing through the surcharge, which is of depth h. If the angular velocity is $\dot{\alpha}$, the rate of work

done by external forces is:

$$P^u \frac{b}{2}\dot{\alpha} - bhw \frac{b}{2}\dot{\alpha} \tag{53}$$

while the rate of internal energy dissipation is:

$$c\, b\dot{\alpha}\, \pi b + c\, b\dot{\alpha}\, h \tag{54}$$

Note that the rate of work done by the weight of the body is zero since its motion is perpendicular to the direction of its own weight. Equating the rate of internal and external work will yield Equation (50), the first limit equilibrium solution. The solution reduces, for the important case of h=0, to p=6.28c.

It is apparent that since the two solutions agree, the first limit equilibrium mode has produced a solution which is an upper bound. Both solutions are applicable for smooth or rough bases, since the mechanism of the upper bound does not require relative motion between the punch and the rotating soil mass.

Different mechanisms may be employed to reduce the upper bound. One such mechanism is shown in Fig. 20b. Using the upper bound technique, the rate of external work includes terms due to the force P moving downward with velocity V, the triangular mass moving diagonally upward (a 45° right triangle is assumed), and the surcharge being pushed upward by the triangular soil mass, while the soil under the footing may

be considered to be many rigid triangles, as in Fig. 7a, sliding past one another in a zone of radial shear. The rate of external work is:

$$\underset{\triangle BOC}{} \quad \underset{\square OCED}{} \quad \underset{\text{AOB}}{} \qquad p^u V - \frac{b^2}{2} w V - bhw V + \frac{b^2}{2} wV \tag{55}$$

The rate of internal energy is dissipated along the quarter circle circumference, within the quarter circle by shearing deformation (it was shown previously that these two terms are equal), along the diagonal shear plane, by shearing through the surcharge, and by relative shearing between the quarter circle and the triangular mass (due to a relative velocity). Therefore:

$$\underset{\text{AOB}}{} \qquad \underset{BC}{} \qquad \underset{CE}{} \qquad \underset{OB}{} \qquad 2c V \frac{\pi b}{2} + c \sqrt{2V} \sqrt{2b} + c V h + c V b \tag{56}$$

equating the rate of internal and external work yields

$$p^u = \frac{P^u}{b} = c \left(\pi + 3 + \frac{h}{b}\right) + wh \tag{57}$$

when h=0, the ultimate bearing capacity is

$$p^u = 6.14c \tag{58}$$

The improvement of the previous limit analysis solutions is only about 2 percent.

Fig. 20c illustrates another failure mechanism. With reference to the figure, the ultimate bearing capacity is given as:

$$p^u = 6c + c\frac{h}{b} + wh \tag{59}$$

which is slightly better than the previous answer. It is apparent that the limit analysis provides the consistent upper bound solutions while the limit equilibrium analysis cannot; when the failure modes, that can be compared, are considered in the solutions.

Figure 21 shows two examples of rigid block sliding separated by velocity discontinuities, approximating the familiar Prandtl and Hill mechanisms, respectively[29]. An infinite variety of such mechanisms can be drawn for this problem or for any other in accord with the intuitive feeling of the designer or analyst for the appropriate mode of failure.

Fig. 21a shows a solution which is only appropriate for a smooth punch, since relative motion is required between the punch and the material. The ultimate bearing capacity is given as

$$p^u = 5.78c$$

A similar mechanism is illustrated in Fig. 21b, although no relative velocity occurs between the punch and the material, and the solution is valid for a rough punch. The ultimate bearing capacity for this case is also

$$p^u = 5.78c$$

The two solutions just illustrated are actually approximations of the well known Hill (See Fig. 21c) and Prandtl (See Fig. 21d) solutions. Both yield the following

$$p^u = (2 + \pi)\ c$$

Since the solutions for a perfectly rough and a perfectly smooth punch are identical, the roughness of the punch does not affect the bearing capacity.

This, then, illustrates the power and simplicity of the limit analysis approach. Although the Hill and Prandtl solutions are not very difficult, they might not be the first to come to mind. The rotating soil mass ($p^u = 6.28c$) or the two wedges ($p^u = 6c$), however, are choices that readily come to mind. Yet, they are only 22% and 17% in error, respectively. Moreover, the bearing capacity of the rotating soil mass may be reduced by shifting the center of rotation. If the center is shifted to 0', as illustrated in Fig. 22a, the rate of external work is:

$$P(r\cos\theta - \tfrac{1}{2}b)\dot{\alpha} \qquad (60)$$

where r is the radius of the discontinuity surface and θ the angle between the face of the punch and the line A0'.

The rate of internal work is given by

$$(\pi-2\theta)\ r\ c\ r\dot{\alpha} \tag{61}$$

and the resulting upper bound solution is:

$$p^u = \frac{c(\pi-2\theta)\ r^2}{r\cos\theta - \frac{1}{2}b} \tag{62}$$

The upper bound may be reduced by minimizing the solution with respect to the variables θ and r:

$$\frac{\partial p^u}{\partial r} = 0$$

and (63)

$$\frac{\partial p^u}{\partial \theta} = 0$$

Hence:

$$b = r\cos\theta_{cr} \tag{64}$$

and

$$b = r\ [2\cos\theta_{cr} - (\pi-2\theta_{cr})\sin\theta_{cr}] \tag{65}$$

Equation (64) states that the location of the center of rotation 0' is directly above 0 as shown in Fig. 22b. Equating Eq. (65) yields

$$\cos\theta_{cr} = (\pi - 2\theta_{cr})\sin\theta_{cr} \tag{66}$$

Introducing this relation into Eq. (62) yields

$$p^u = \frac{P}{b} = \frac{4c}{\sin 2\theta_{cr}} \tag{67}$$

θ_{cr} can be determined from Eq. (66). This is found to be:

$$\theta_{cr} = 23.2^\circ \tag{68}$$

and

$$p^u = 5.53c \tag{69}$$

which agrees with Fellenius' solution[22].

Although the upper bounds, p^u = 6.28c, 6.14c, 6c, 5.78c, 5.53c, are not extremely close to the actual answer $(2+\pi)c$, they are obtained quickly and easily. Each can provide useful information when the exact answer is not available and each can prove even more valuable when the soil being loaded is inhomogeneous and so not easily amenable to exact solution.

5.3 Plastic Limit Analysis--Lower Bounds

To obtain a lower bound of the bearing capacity problem by limit analysis, choose a simple stress field, which gives 2c as a lower bound, as shown in Fig. 23a. Since a hydrostatic pressure has no effect

on plastic yielding for soils with $\emptyset=0$, the simple addition of the hydrostatic pressure 2c+wh as shown in Fig. 23b to Fig. 23a increases the ultimate load to (Fig. 23c):

$$p^{\ell} = 4c + wh \tag{70}$$

which is an improved lower bound, but not a very good one.

Now, a little physical intuition will raise the lower bound to a very useful point. Experience has shown that the load on soil "spreads", or is carried by an even greater area, the deeper one goes (See Fig. 24a). Therefore, consider the stress field, shown in Fig. 24b, consisting of two inclined "legs" of 2c each. Where they meet, under the punch, there is a vertical component of 3c and horizontal component of c. If the stress field of Fig. 23b are superposed onto the field of Fig. 24b, the stress field shown in Fig. 24c results and it is easily verified that the superposition of these stress fields does not violate the yield condition anywhere. Therefore:

$$p^{\ell} = 5c + wh \tag{71}$$

This lower bound may be improved through a more judicious choice of stress fields. Valuable techniques for constructing lower bounds of this "truss-like" nature have been developed by Drucker and Chen[30]. It was shown in their paper that the familiar Prandtl field may be imagined physically as a load supported by infinitely many supporting

legs. A picture of 9 vertical and inclined legs at 10° to each other is shown in Fig. 25. As the number of legs grows, the stress in each decreases. In the limit, the Prandtl field beneath the footing is recovered. Figure 24c shows clearly that the three legs's approximation for the Prandtl field gives the answer sufficiently accurate for practical purpose.

In order to avoid obscuring the basic points, the discussion, up until now, has been limited to a cohesive soil (ϕ=0) so that the Coulomb's yield criterion of soil plasticity is reduced to the familiar Tresca yield criterion of metal plasticity. The extension of the above discussion to include c-ϕ soil is evident. The details of such development has been discussed by Chen[21].

5.4 Limit Analysis of Three Dimensional Problems

In this section, upper and lower bounds are obtained for the ultimate bearing capacity of square and rectangular footings on a cohesive soil (ϕ=0).

A simple failure mechanism for the footing is shown diagrammatically in Fig. 26. A-E-E'-A' is the area of footing and the downward movement of the footing is accommodated by movement of the material as indicated in Fig. 26a. In Fig. 26b is shown the plan and section in Fig. 26a, and it can be seen that this mechanism is an extension into three dimensions of a simple modification of the two-dimensional Hill's

mechanism in Fig. 21c.

The internal dissipation of energy on the discontinuous surface A-B-C-D-D'-C'-B'-A' and in the radial shear zone E-B-C-C'-E'-B' is:

$$2\ c\ v\ \frac{ba}{\sqrt{2}} + 2\ c\ v\ \frac{b}{\sqrt{2}}\ \frac{\pi}{2}\ a \qquad (72)$$

Energy dissipated on the two end surfaces A-B-C-D-E-A and A'-B'-C'-D'-E'-A' is:

$$2\ c\ v\ \frac{b}{\sqrt{2}}\ \frac{b}{\sqrt{2}} + 2\ c\ v\ \frac{\pi}{4}\ \frac{b^2}{2} \qquad (73)$$

Energy dissipated through the surcharge is:

$$c\ \frac{v}{\sqrt{2}}\ ah \qquad (74)$$

while the rate of external work is $Pv/\sqrt{2} - wabhV/\sqrt{2}$. Hence, the resulting ultimate bearing capacity is:

$$p^u = \frac{P^u}{ba} = c\ \left(5.14 + 2.52\ \frac{b}{a} + \frac{wh}{c}\right) \qquad (74)$$

Thus, for a square footing, for which b=a, Expression (74) gives the value 7.66c + wh and a value of 5.77c + wh is found for a ratio b/a = 4. This expression tends to the value of 5.14 c + wh for rectangles whose

length is great compared with their breadth, in agreement with the familiar Prandtl's solution for the two-dimensional footing.

Considering next the lower bound, a three-dimensional stress field for the rectangular footing is shown in Fig. 27, which is a direct extension of the two-dimensional stress field in Fig. 23b and Fig. 24b. The stress field of Fig. 27b establishes 3c as a lower bound for the ultimate bearing pressure. It is easily verified that superposition of the stress field of Fig. 27a on that of Fig. 27b does not lead to stresses in excess of the yield limit. Thus, 5c + wh is a lower bound for the ultimate bearing pressure in the three-dimensional rectangular or square footing. The failure mechanism of Fig. 26 and the stress field of Fig. 27, therefore, show that the ultimate bearing pressure for a square footing lies within 21 percent of the value 6.33c + wh.

Further improvement in the upper bound would require the more elaborate failure mechanism discussed by Shield and Drucker[31]. It was found that the value 5.71c + wh is a better upper bound for the square footing then those obtained previously.

6. CONCLUSIONS

Although a soil with cohesion c and internal friction $\emptyset$ is not modeled accurately by a theory of perfect plasticity, it is of interest to note that many classical solutions of stability problems in soil mechanics can be obtained by limit analysis technique. Within the framework of the idealizations, the limit analysis approach is rigorous and the techniques are competitive with those of limit equilibrium, in some instances being much simpler. It should be kept in mind, however, that too much should not be expected of the perfect plastic assumption for such a complicated heterogeneous substance as soil. Predictions based on this assumption on other problems in soil mechanics may be misleading. Nevertheless, it seems clear that the perfect plastic assumption is sufficiently good for stability problems in soil mechanics.

7. ACKNOWLEDGMENTS

The results in this paper were obtained in the course of research supported by the Institute of Research of Lehigh University and The National Science Foundation under Grant GK-3245 to Lehigh University.

The authors would like to thank Professor J. W. Fisher for his review of the manuscript, and are indebted to Miss J. Arnold for typing the manuscript and to Mr. J. Gera for the drafting.

8. TABLE AND FIGURES

TABLE 1 COMPARISON OF LATERAL EARTH PRESSURE SOLUTIONS
BY METHODS OF LIMIT EQUILIBRIUM AND LIMIT ANALYSIS

angle of internal friction ϕ	wall friction angle δ	backfill angle β	ACTIVE EARTH PRESS. $k_a = k_{an} \sec\delta$		PASSIVE EARTH PRESS. $k_p = k_{pn} \sec\delta$	
			LIMIT EQUILIBRIUM	LIMIT ANALYSIS	LIMIT EQUILIBRIUM	LIMIT ANALYSIS
10	0	0	.704	.704	1.42	1.42
	10	0	.634	.635	1.65	1.73
20	0	0	.490	.490	2.04	2.04
		10	.569	.566	2.59	2.59
	10	0	.426	.446	2.52	2.64
		10	.507	.531	3.53	3.70
	20	0	.350	.426	2.93	3.52
		10	.430	.516	4.62	5.59
30	0	0	.333	.333	3.00	3.00
		10	.374	.372	4.08	4.09
		20	.441	.439	5.74	5.78
	10	0	.290	.307	3.96	4.15
		10	.334	.350	6.03	6.31
		20	.401	.420	9.94	10.41
	20	0	.247	.297	5.06	6.15
		10	.282	.338	9.05	10.91
		20	.334	.413	19.40	23.37
40	0	0	.217	.217	4.60	4.60
		10	.238	.237	6.84	6.85
		20	.266	.266	11.06	11.10
	10	0	.195	.204	6.63	6.92
		10	.215	.223	11.53	12.08
		20	.242	.253	24.00	25.36

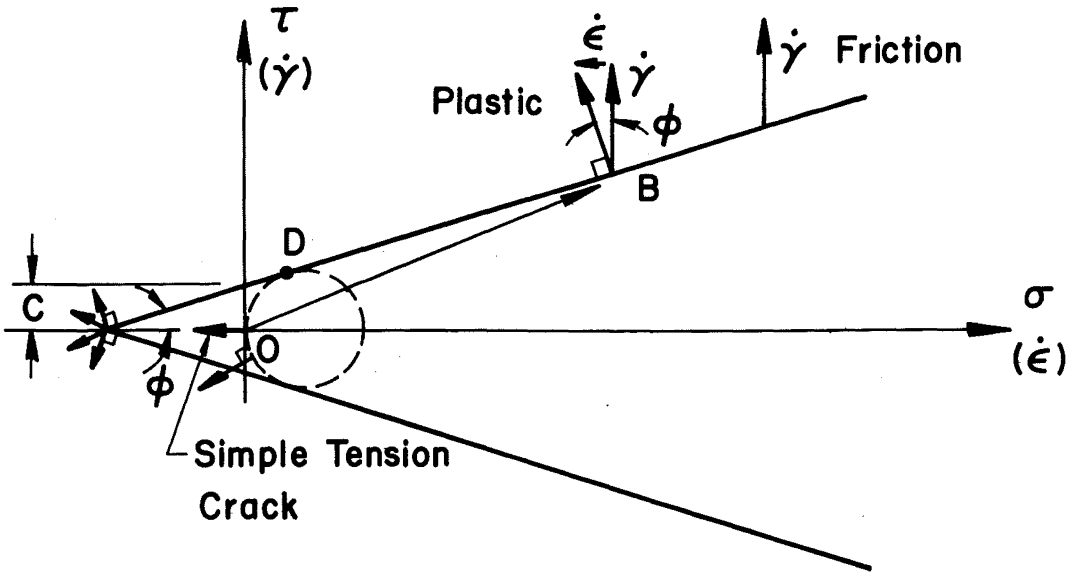

Fig. 1 Plastic Strain Rate is Normal to Yield Curve for Perfectly-Plastic Theory, but Parallel to τ Axis for Frictional Theory

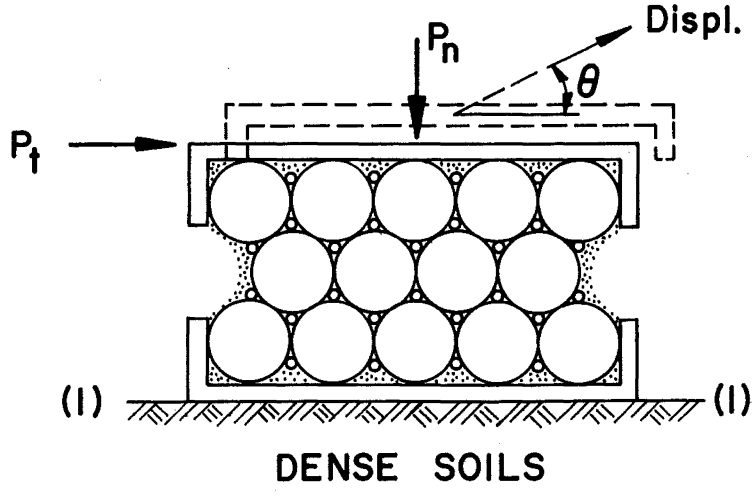

Fig. 2 A Simple Physical Model

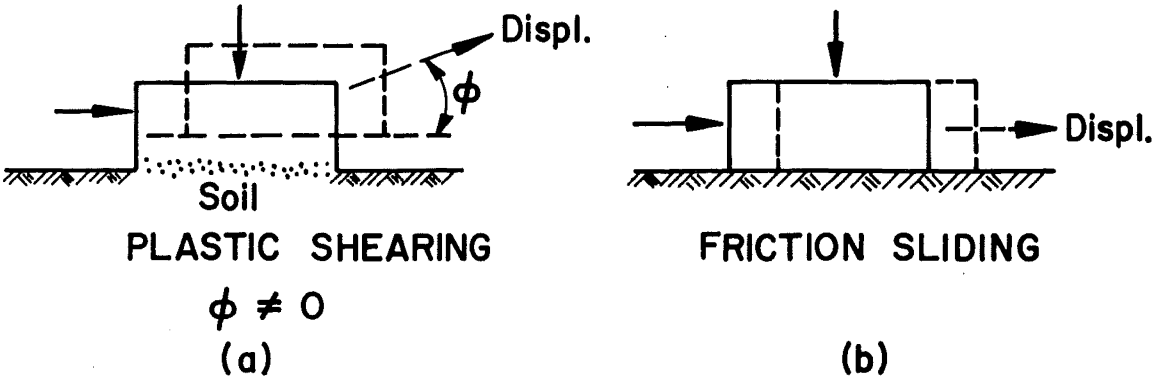

Fig. 3 Difference Between Coulomb Sliding and Coulomb Shear

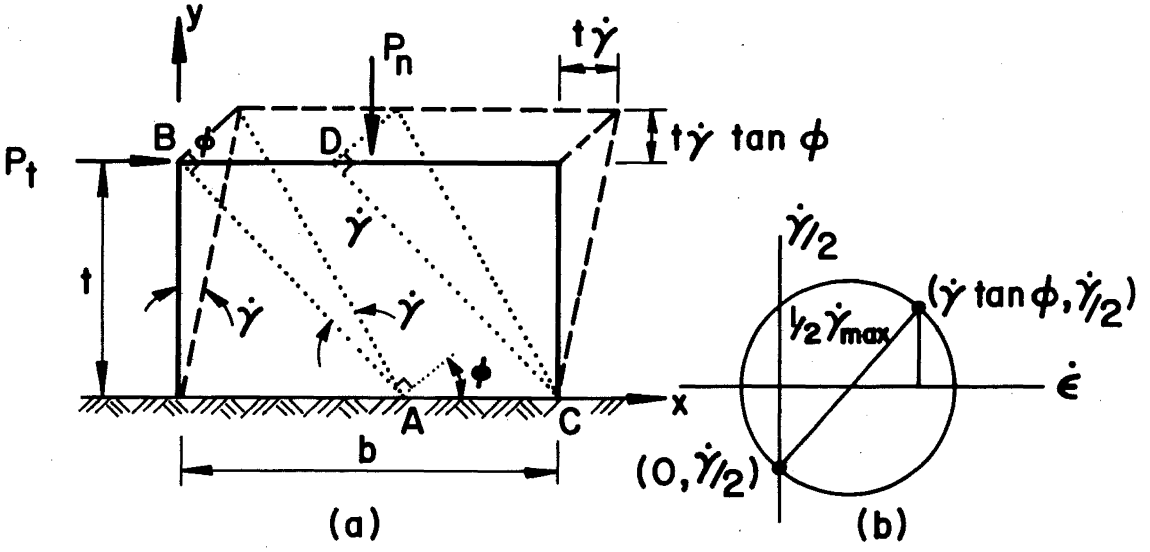

Fig. 4 Dilatation Accompanies Perfectly-Plastic Homogeneous Shearing

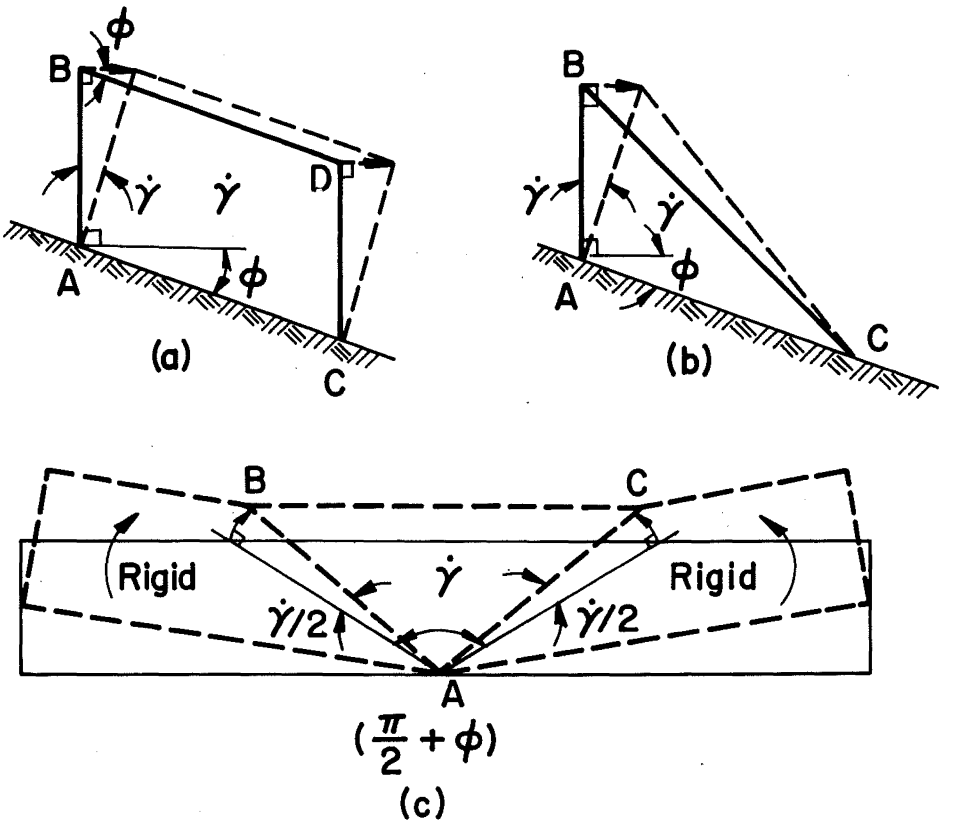

Fig. 5 Homogeneous Shearing Zone with Different Shapes of Mode

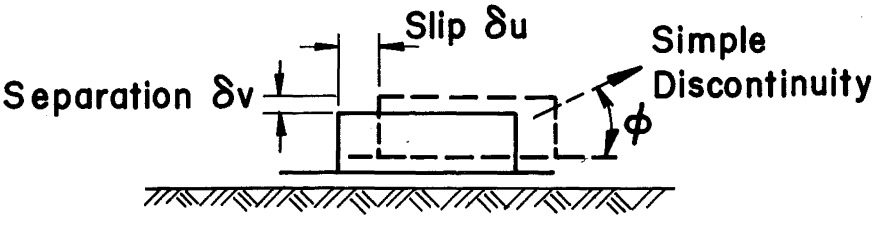

Fig. 6 Narrow Transition Layer

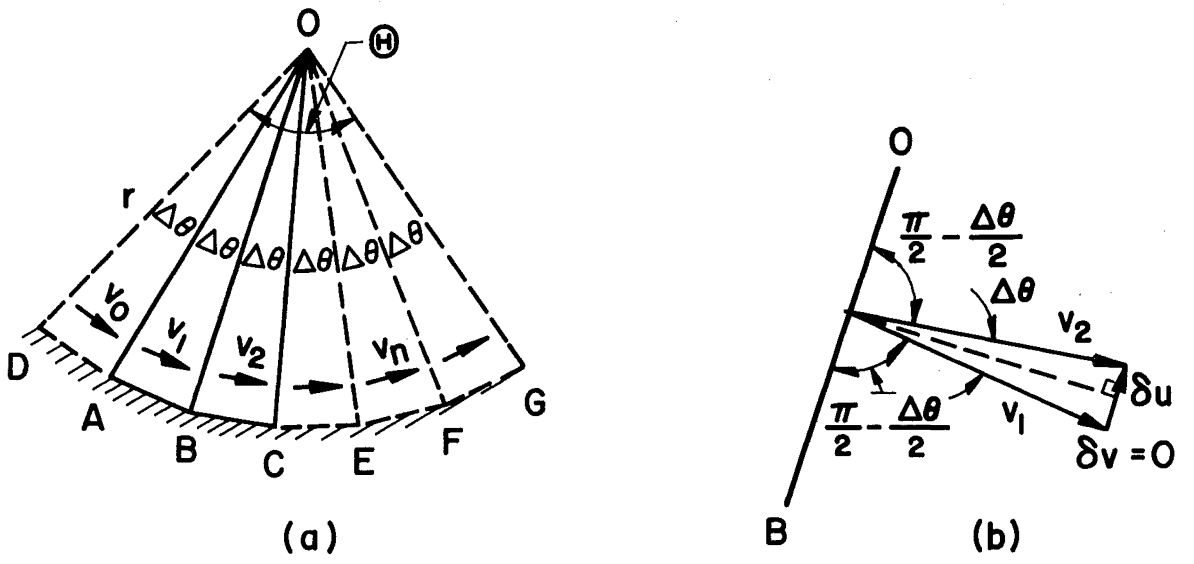

Fig. 7 Rigid Triangles Give Radial Shear Zone in Limit
(a) Energy Dissipated Along the Radial Line O-B is the Same as Dissipated Along the Line A-B
(b) $V_n=V_2=V_1=V_o=V$ True for all Values of $\Delta\theta$

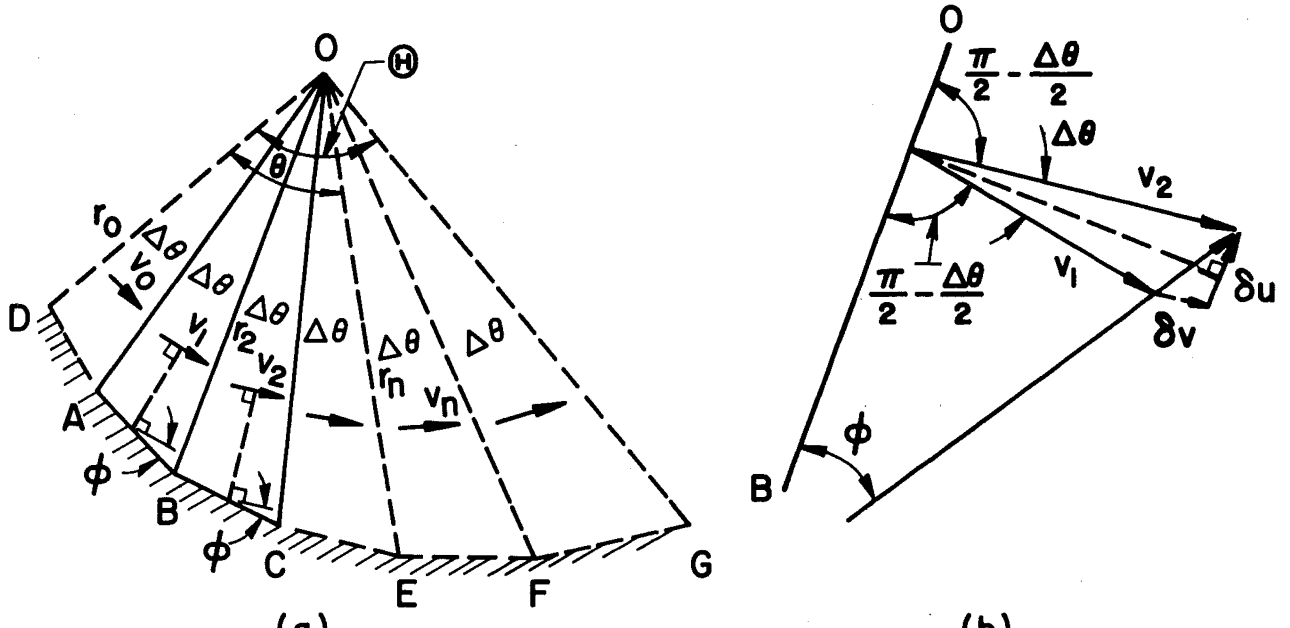

$$r_n = r_o\, e^{\theta \tan \phi}$$

Fig. 8 Rigid Triangles Give Log Spiral Zone in Limit
(a) Energy Dissipated Along the Radial Line O-B is the Same as Dissipated Along the Line A-B
(b) $V_2=V_1(1+\Delta\theta\tan\phi)$ True Only for Samll Values of $\Delta\theta$

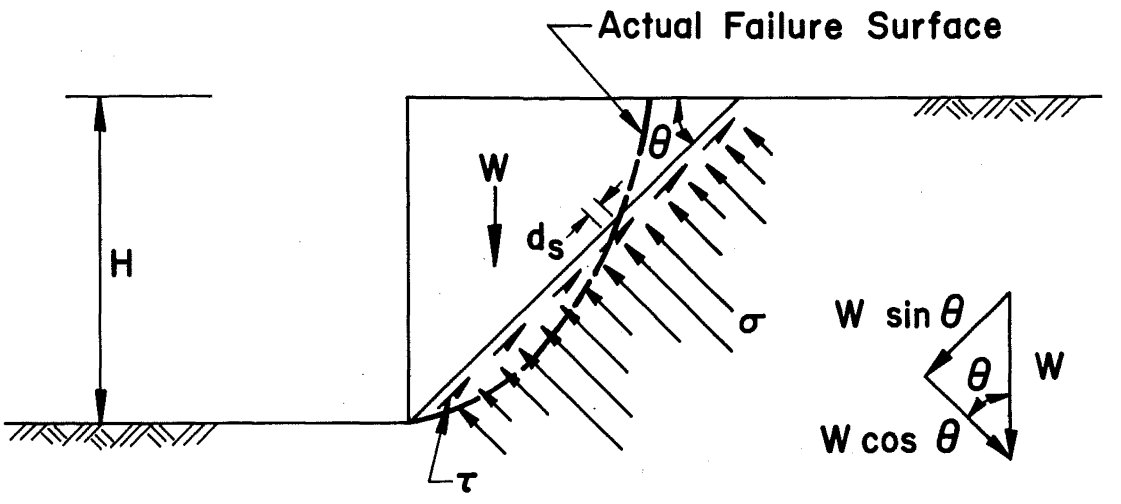

Fig. 9 Limit Equilibrium Solution for the Stability of a Vertical Cut

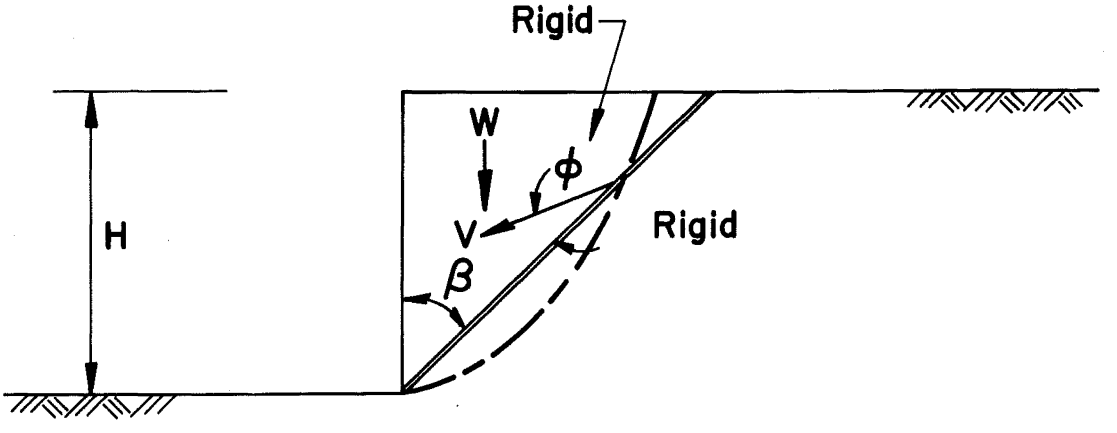

Fig. 10 Limit Analysis Failure Mechanism for the Stability of a Vertical Cut

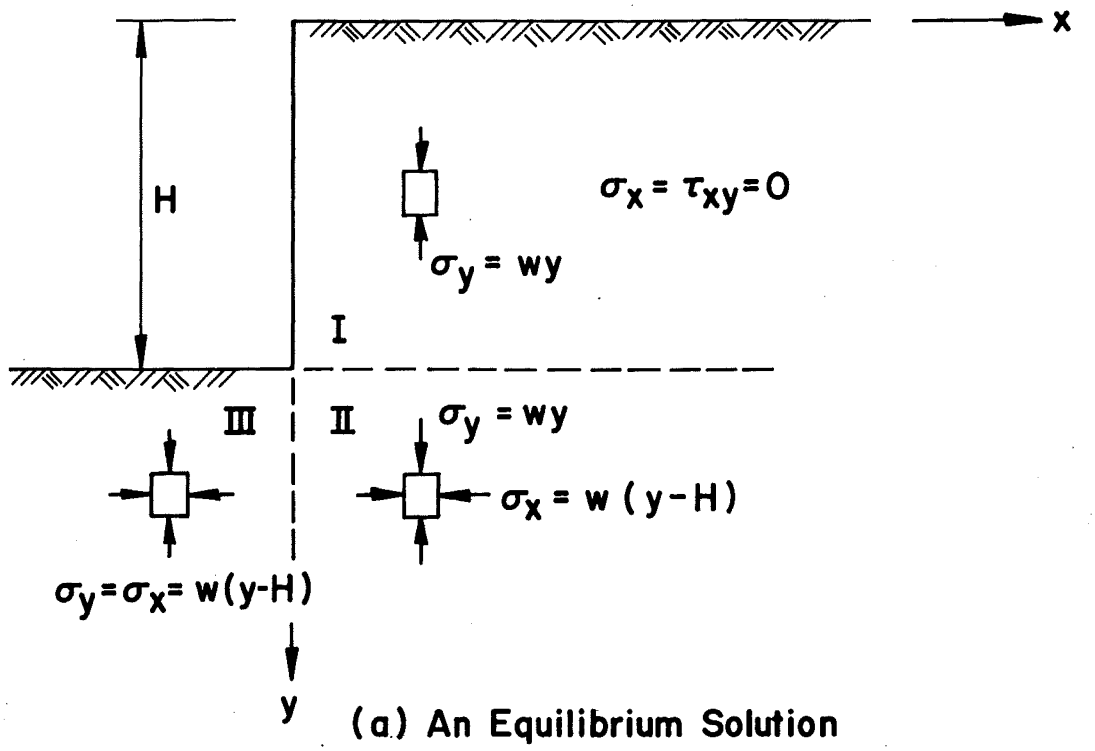

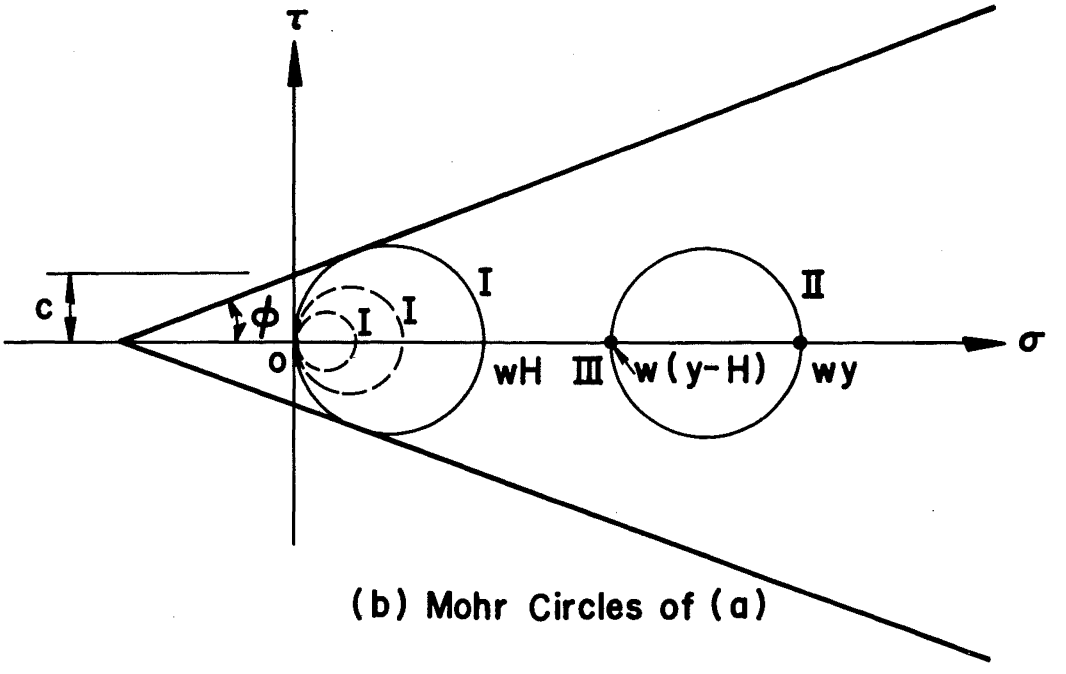

Fig. 11 Limit Analysis Stress Field for the Stability of a Vertical Cut

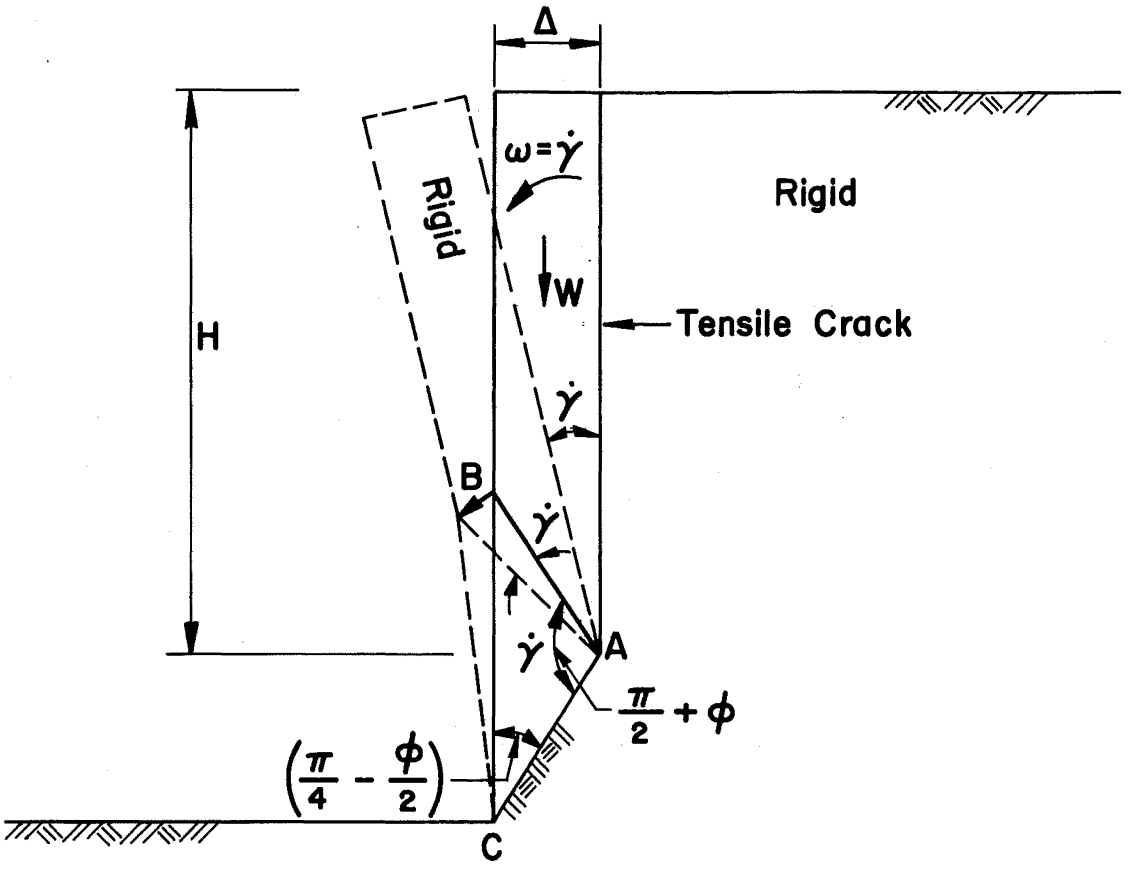

Fig. 12 Rotational Mechanism Containing a Simple Tension Crack and the Homogeneous Shearing Zone of Fig. 5b for Soil Unable to Take Tension

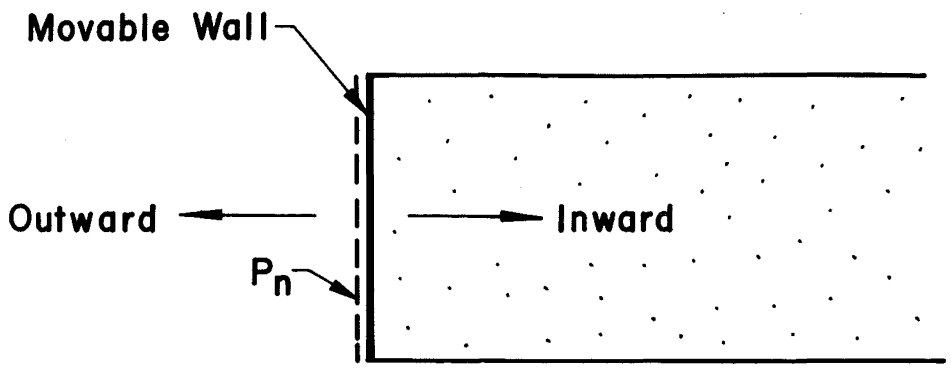

(a) Vertical Section Through Bin

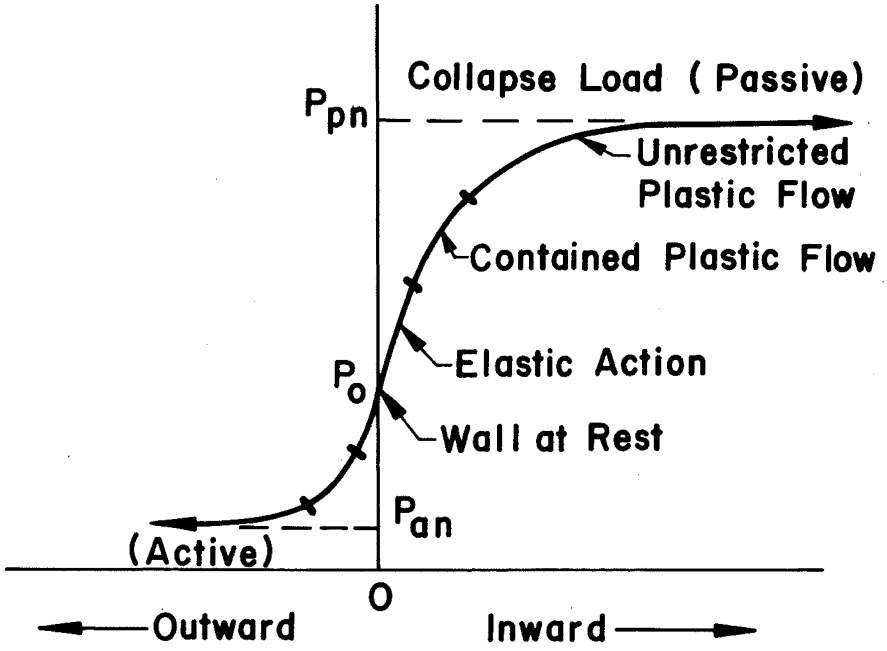

(b) Load Displacement Relationship

Fig. 13 Results of Retaining-Wall Tests

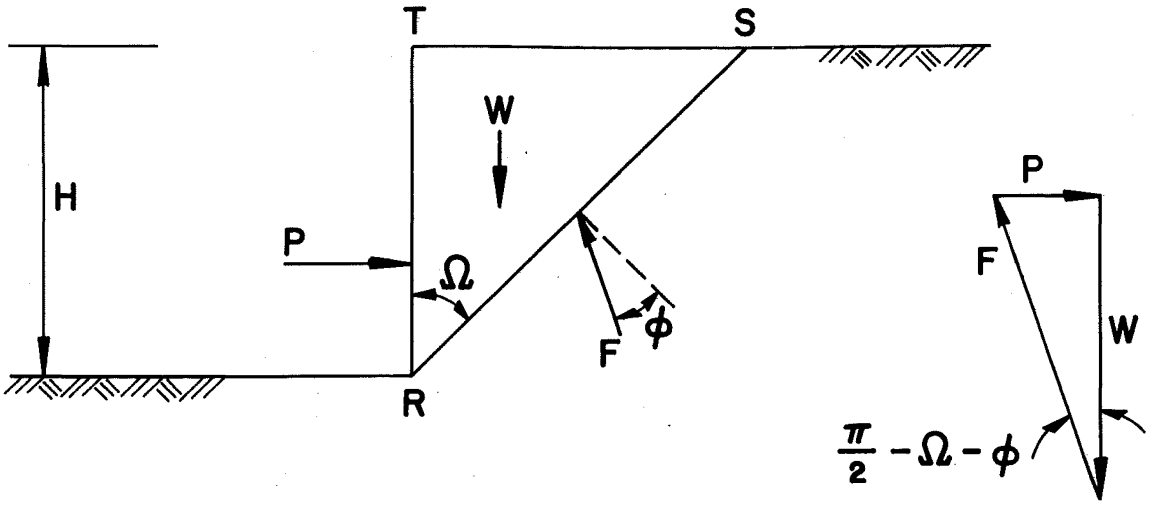

Fig. 14 Limit Equilibrium Solution for Lateral Earth Pressure (Coulomb's Solution)

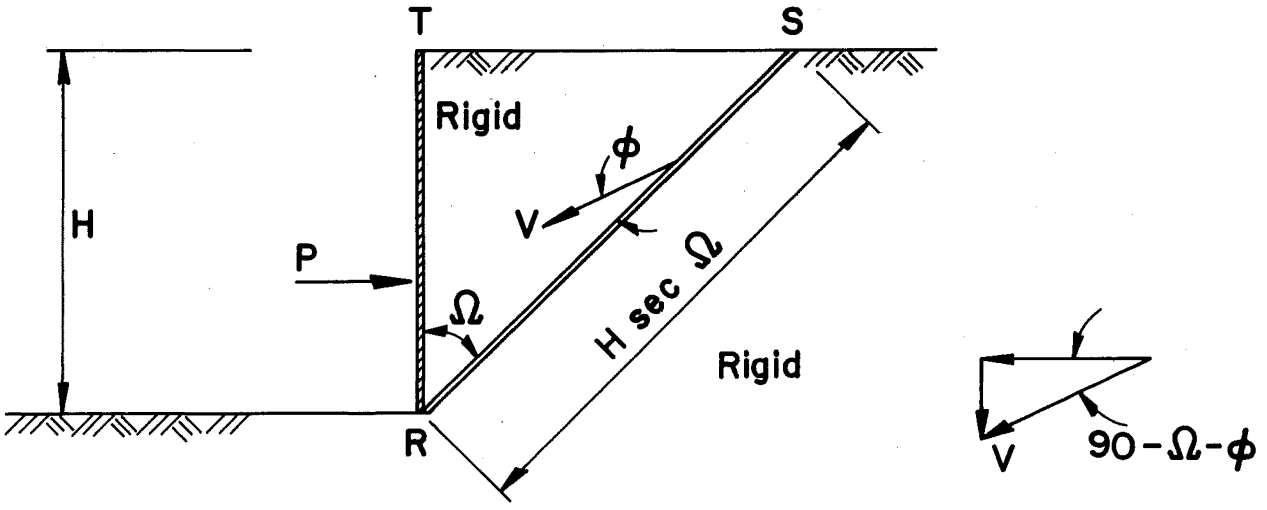

Fig. 15 Limit Analysis Solution for Active Earth Pressure

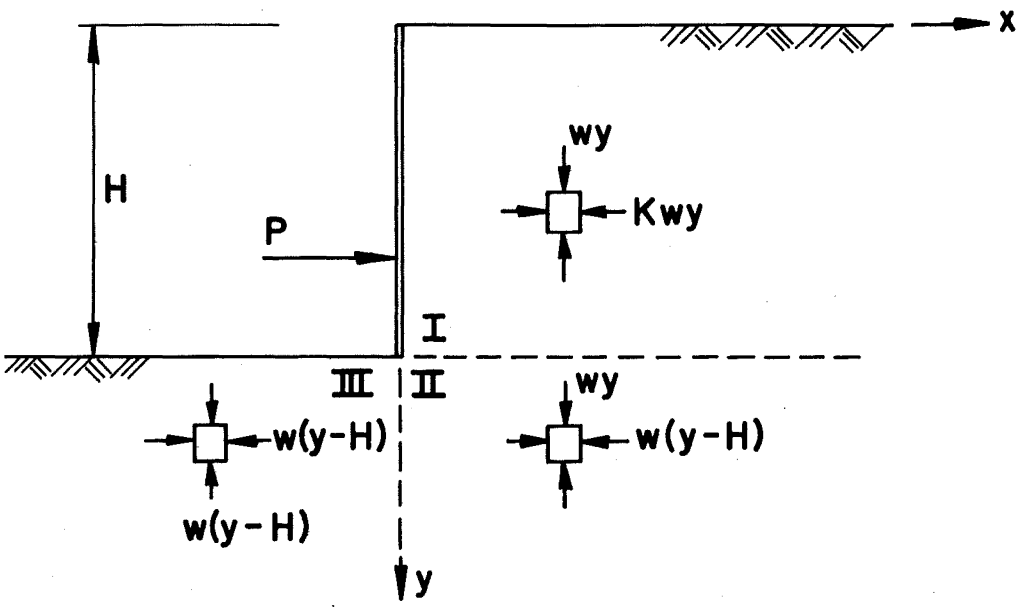

(a) An Equilibrium Solution

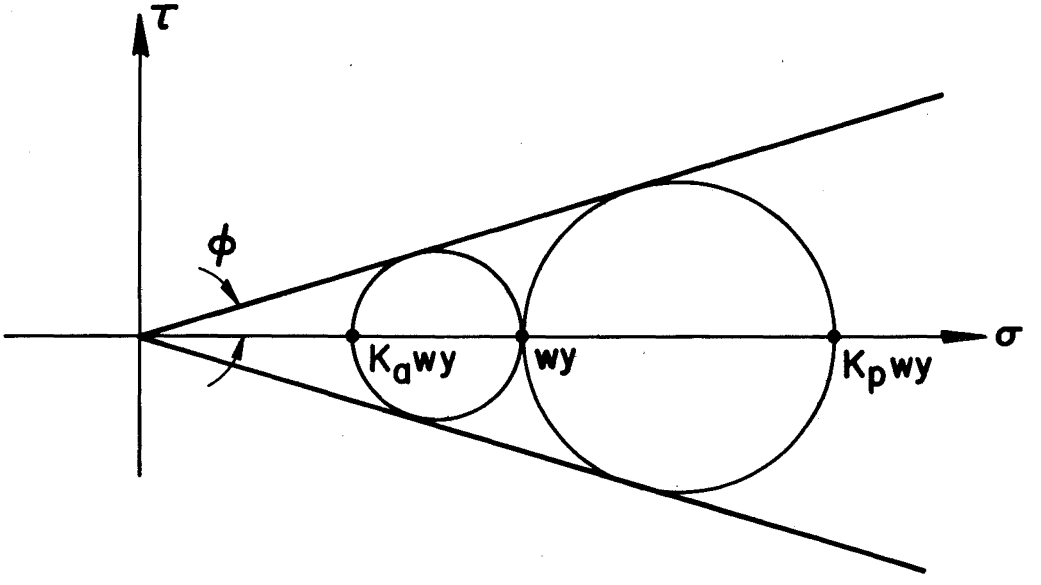

(b) MOHR Circles of Region I in (a)

Fig. 16 Limit Analysis Stress Field for Lateral Earth Pressure

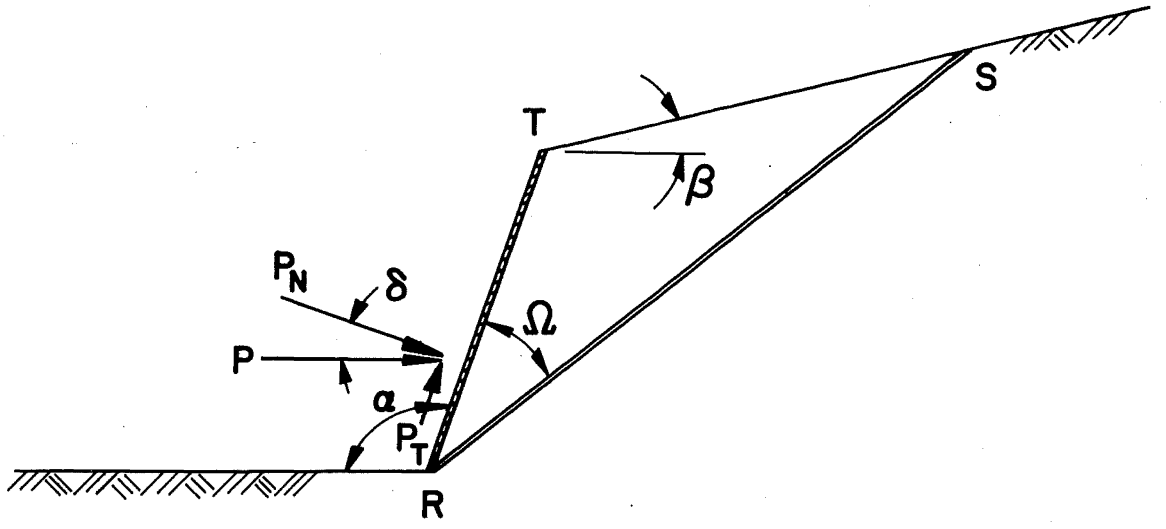

Fig. 17 Plane Sliding for Lateral Earth Pressure Problems in General

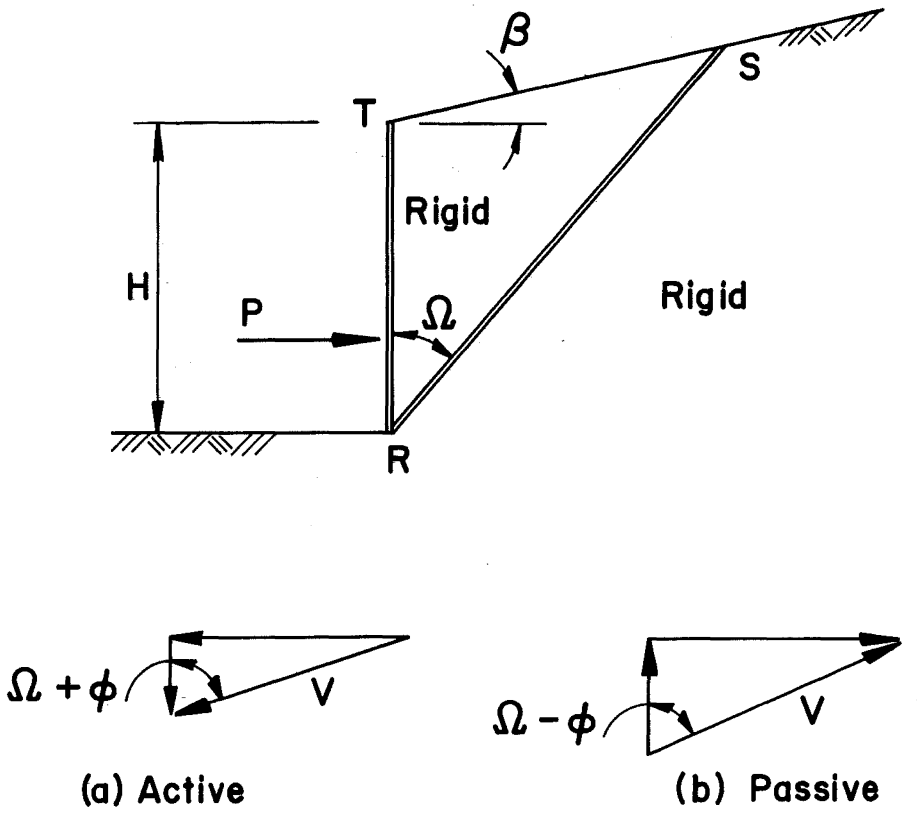

Fig. 18 Active and Passive Lateral Earth Pressures for a Vertical Wall

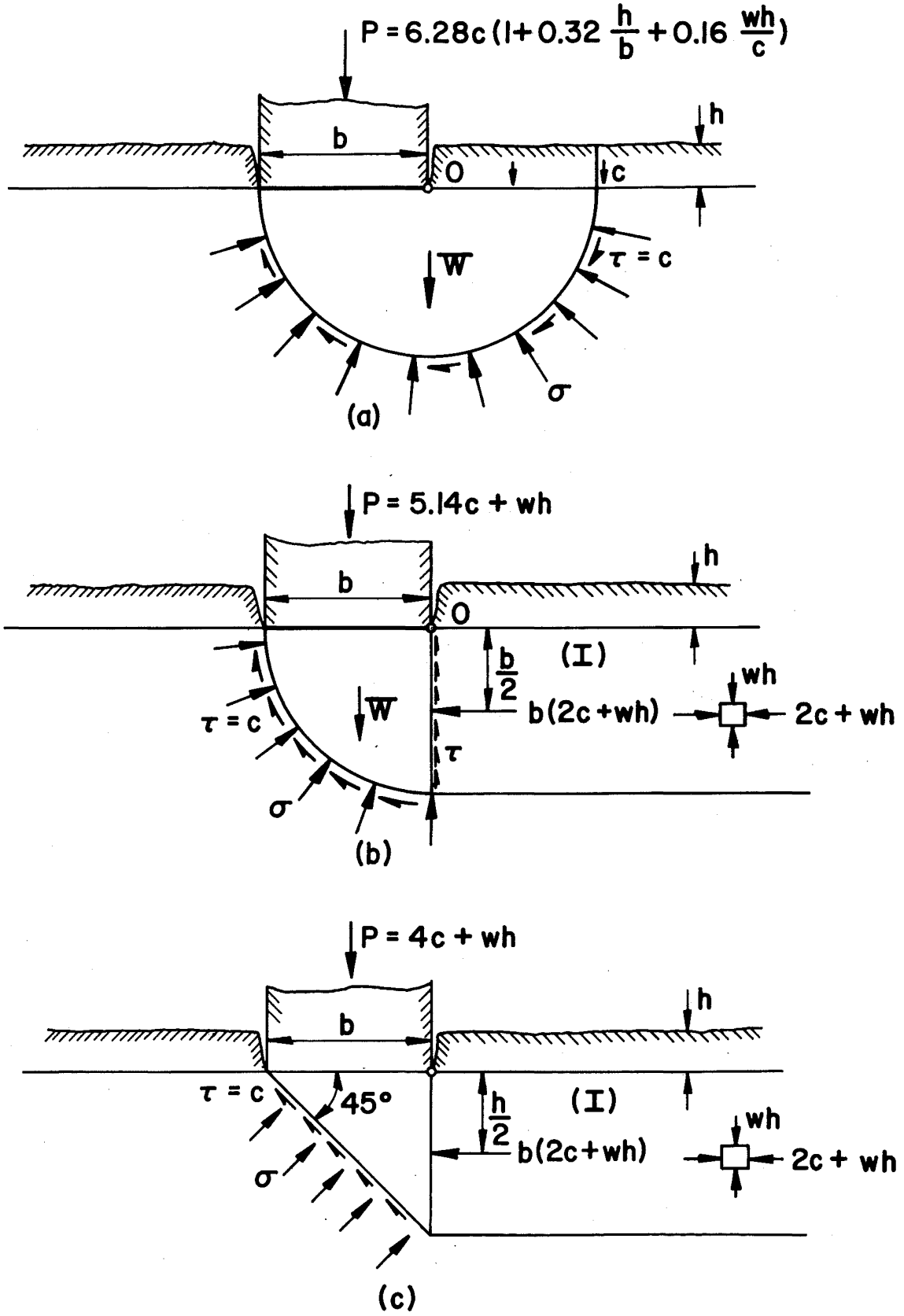

Fig. 19 Limit Equilibrium Modes of Failure, $\phi=0$

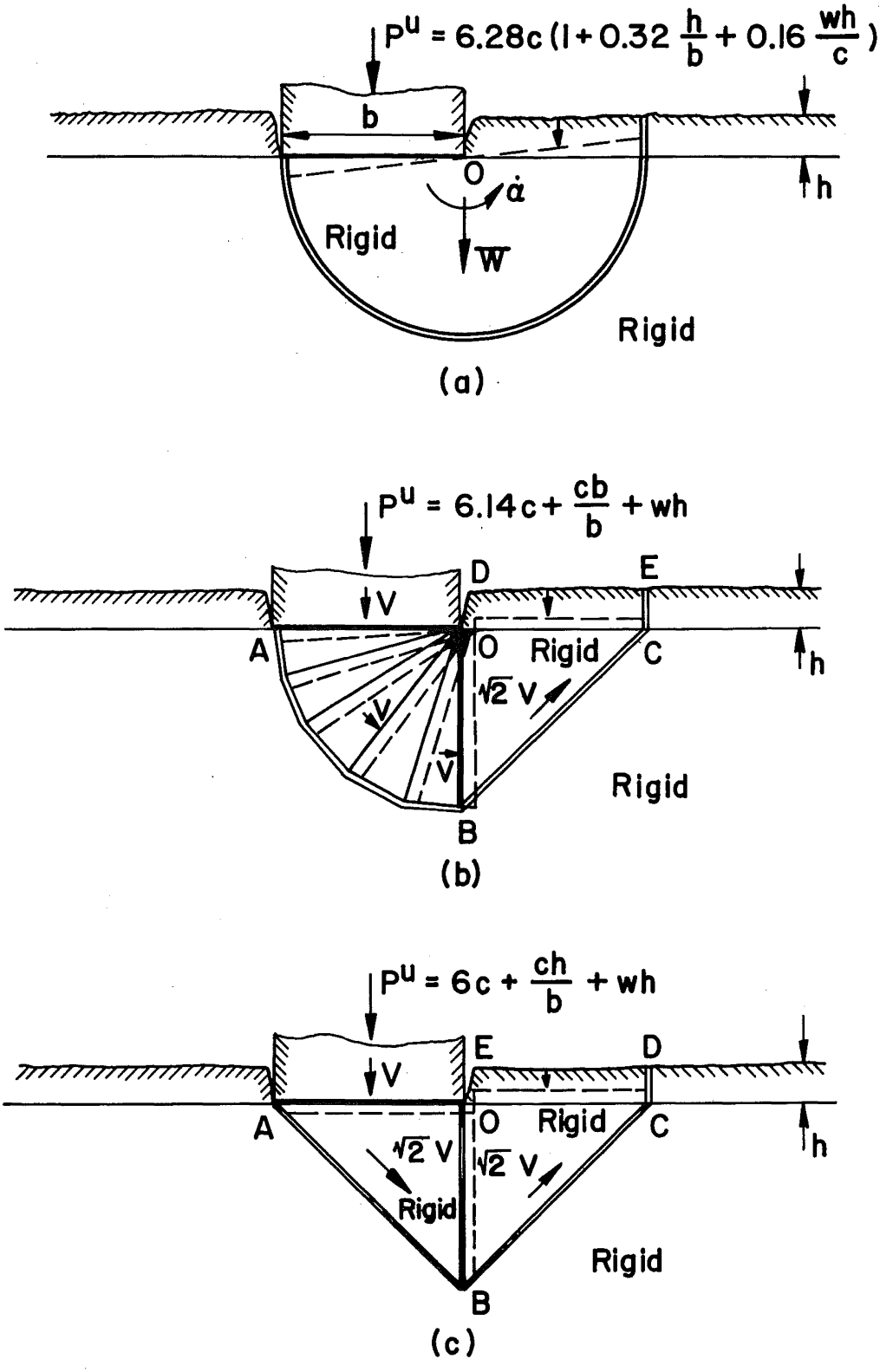

Fig. 20 Limit Analysis Upper Bounds on the Bearing Capacity of Soils, $\emptyset=0$

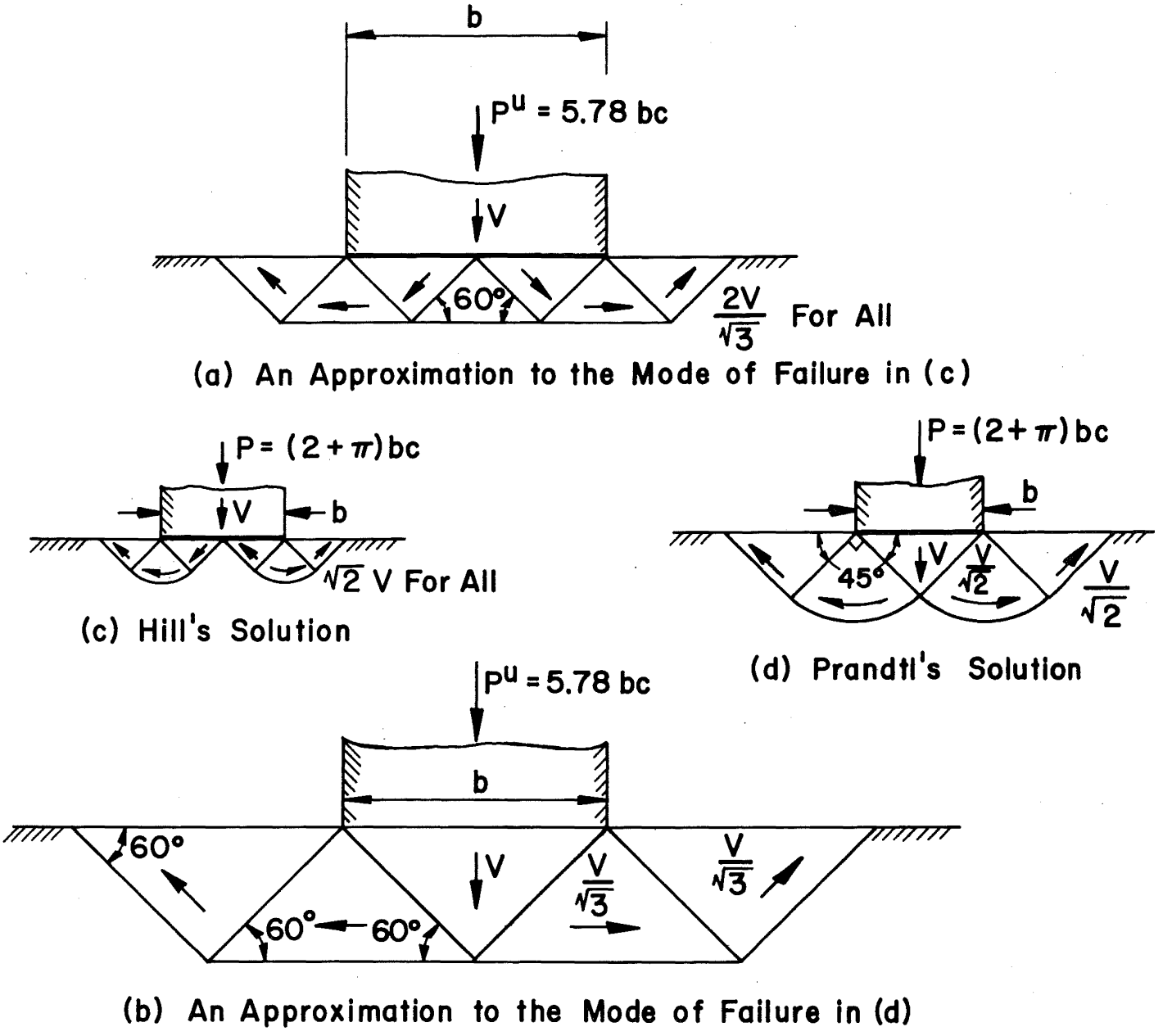

Fig. 21 Rigid Blocks Sliding to Approximate Slip-Line Fields

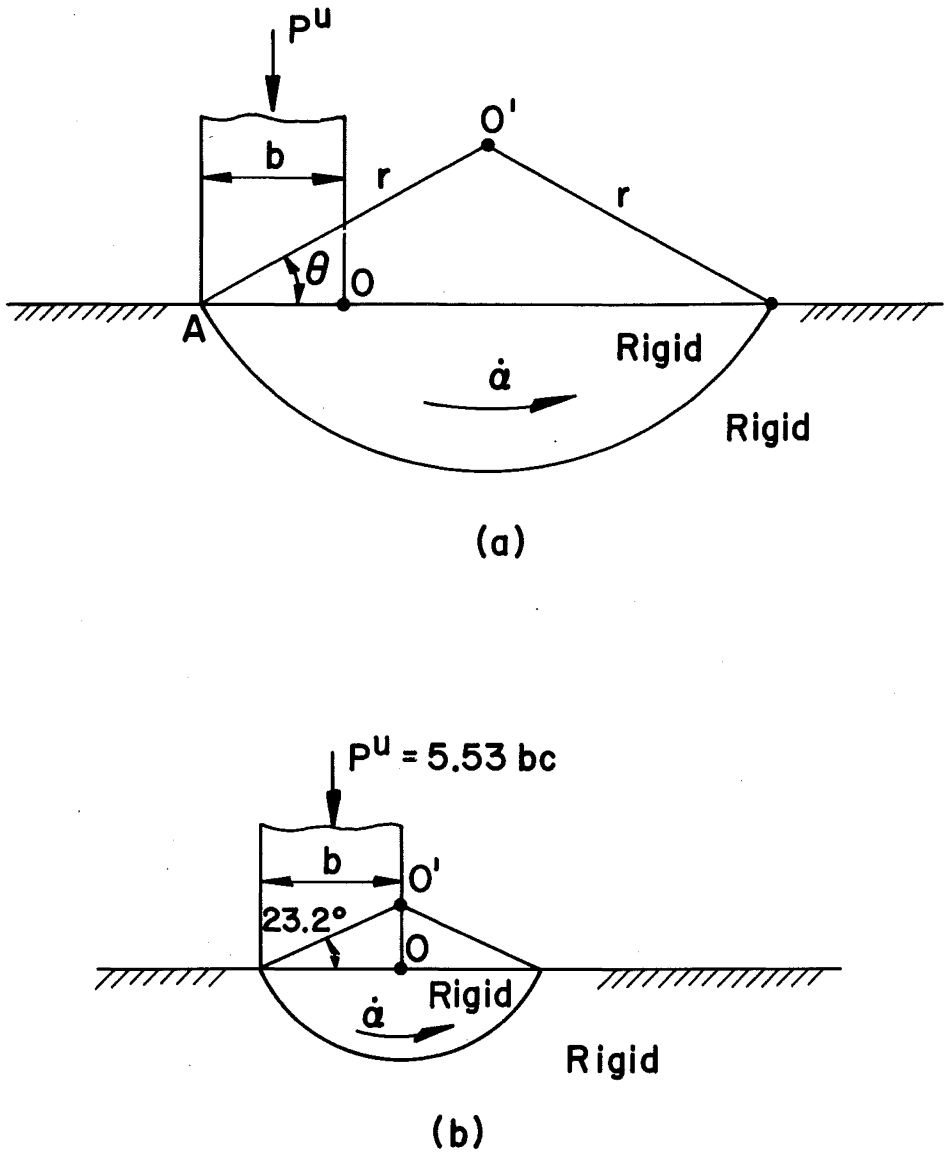

Fig. 22 Rotating Soil Mass with Center at 0' for Purpose of Minimizing Upper Bound

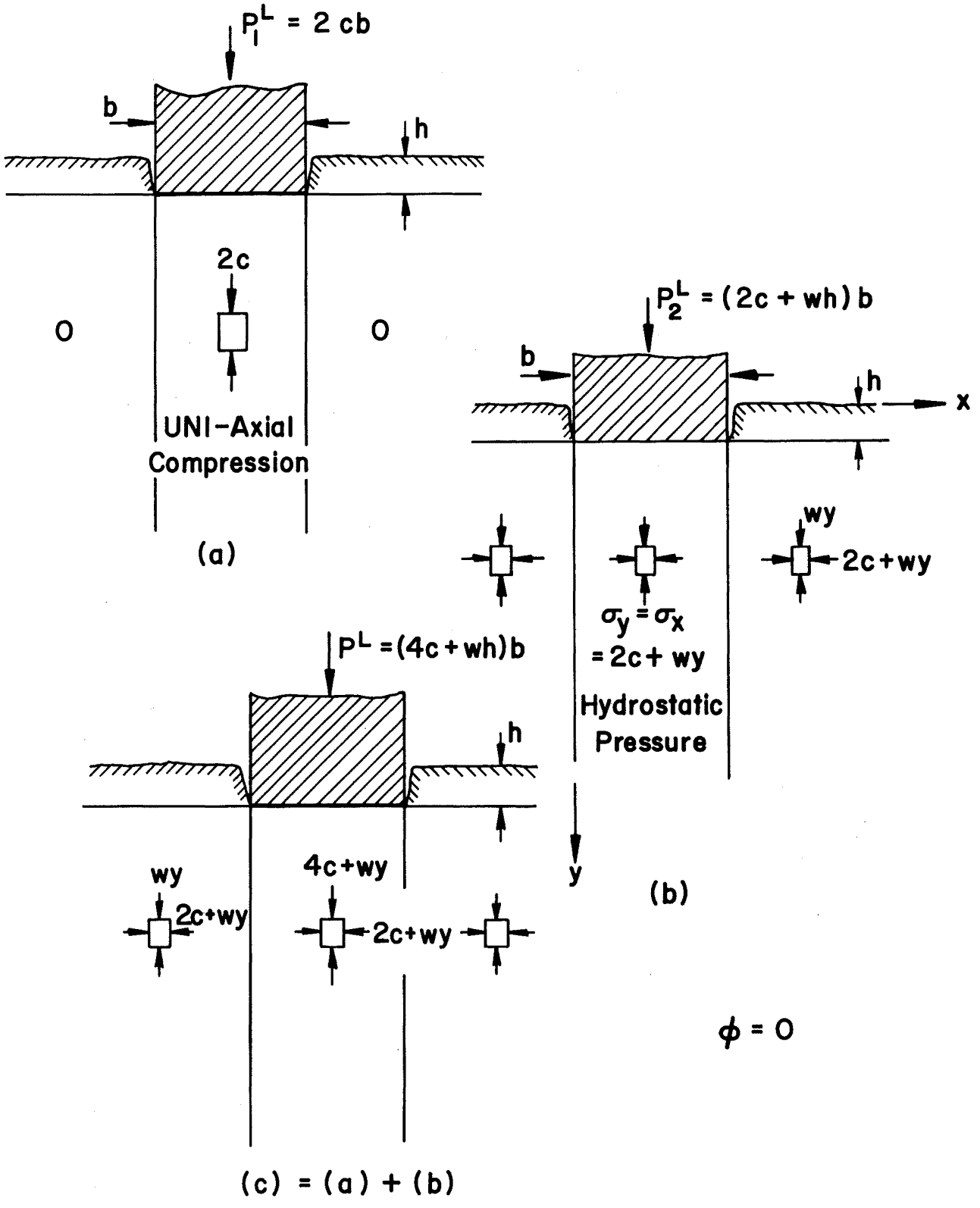

Fig. 23 Limit Analysis Lower Bounds on the Bearing Capacity, Stress Field (c) is the Simple Addition of the Stress Fields (a) and (b)

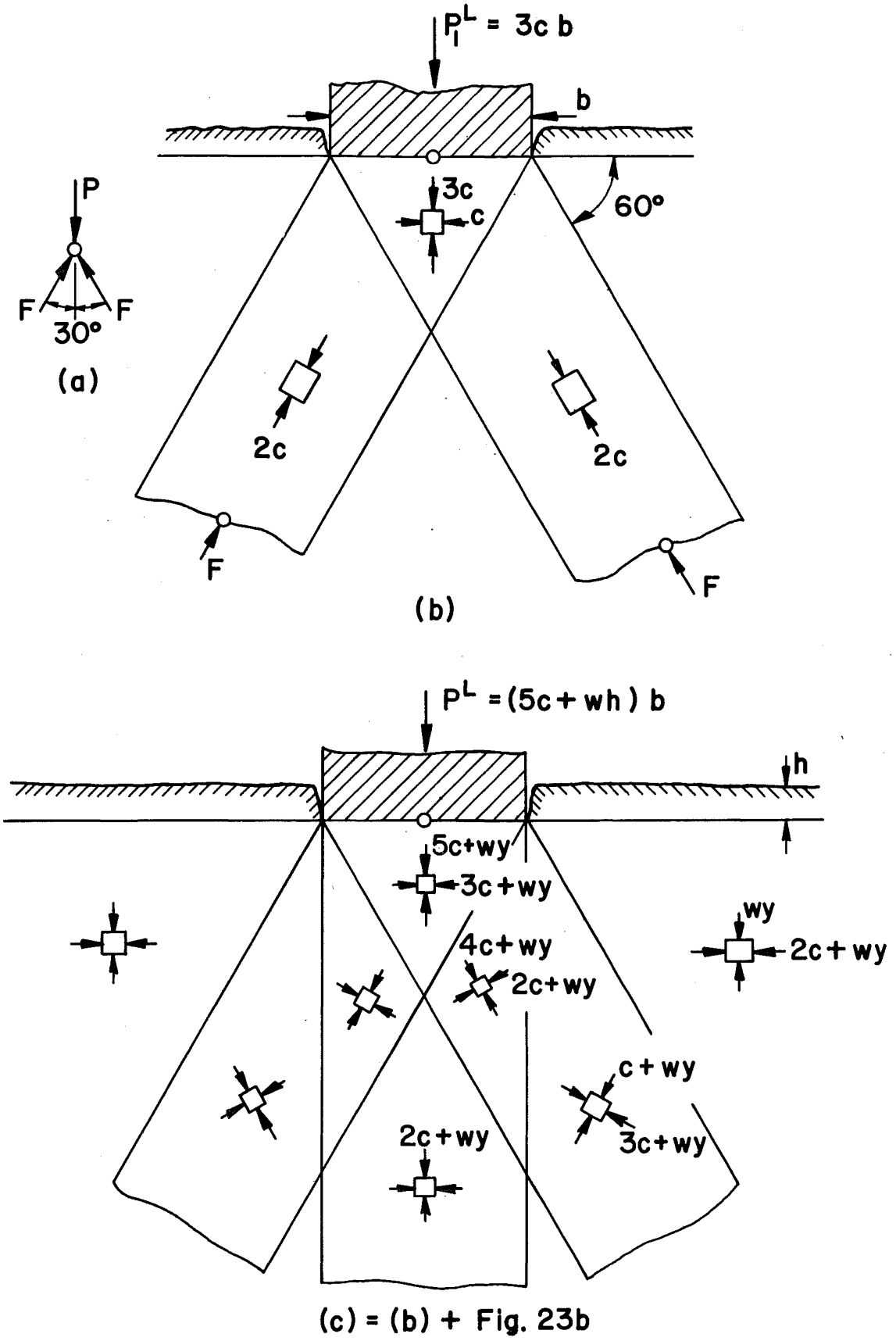

Fig. 24 Limit Analysis Lower Bounds: Stress Field (c) is the Result of Adding the Stress Fields in (b) and in Fig. 23b

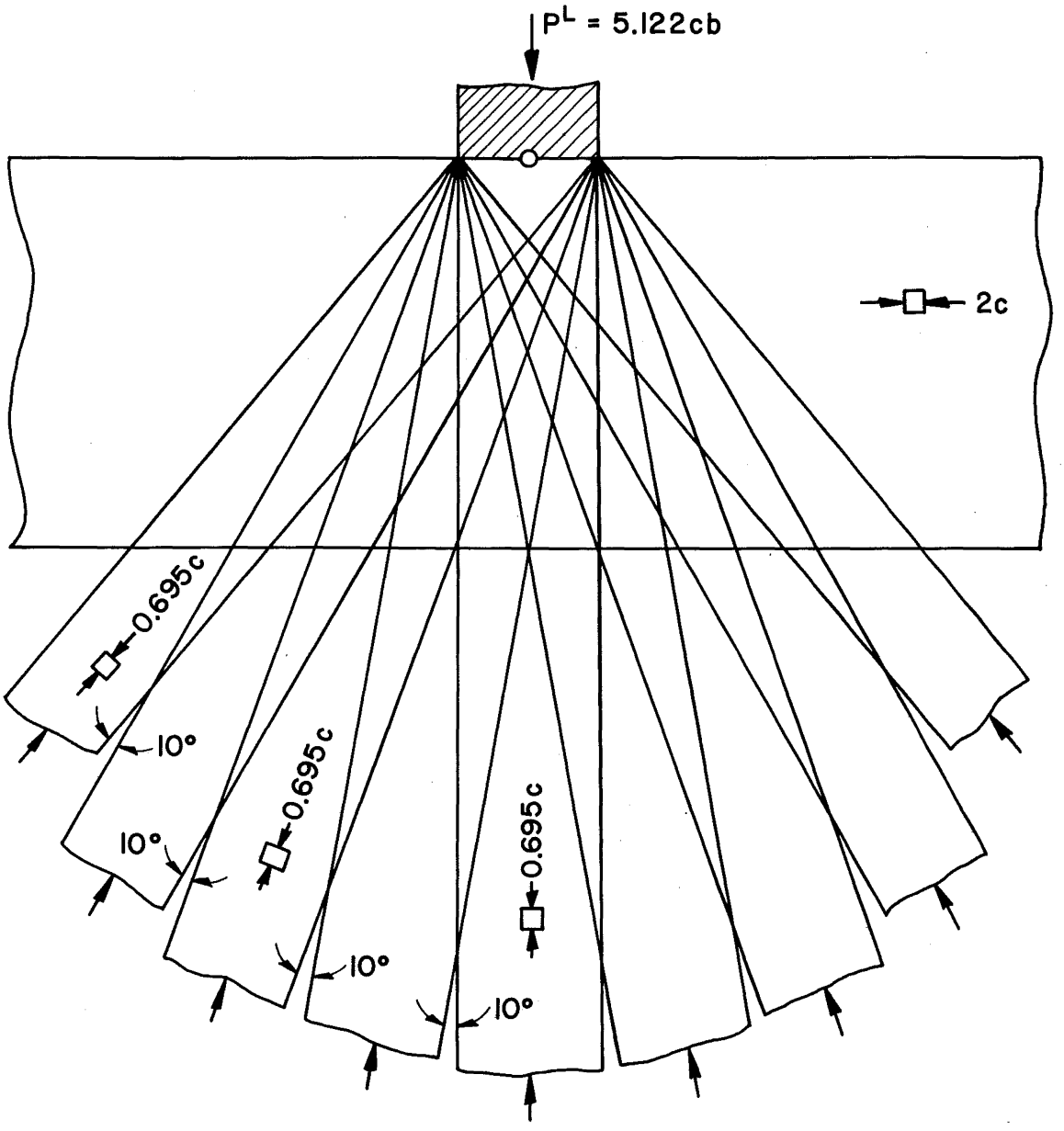

Fig. 25 Supporting Legs Give Prandtl's Solution in Limit

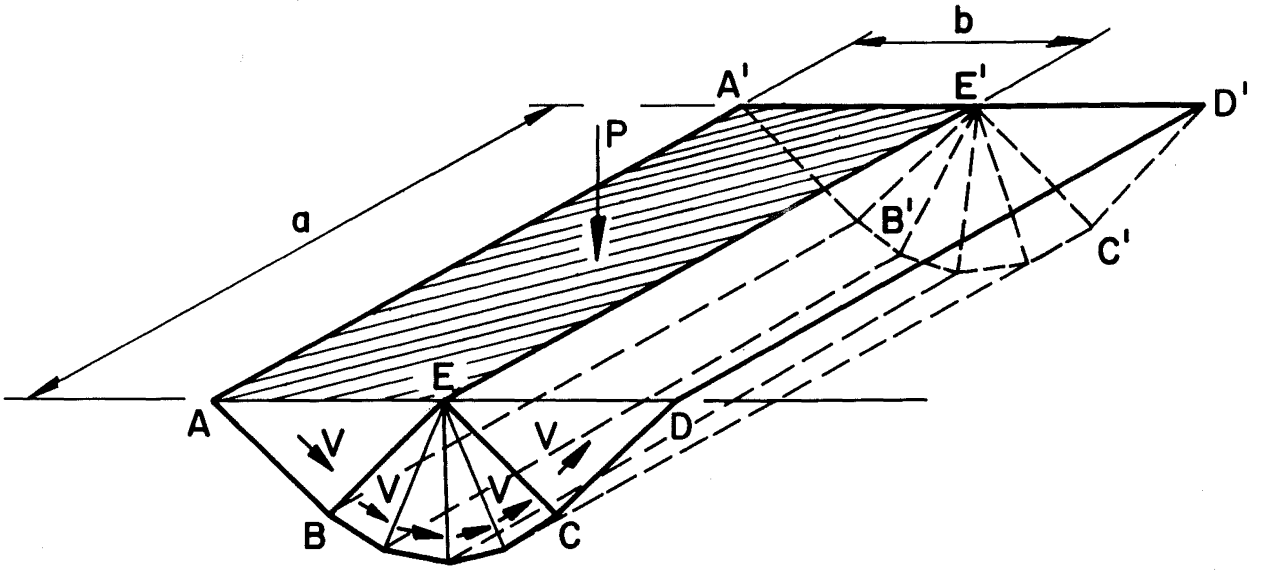

(a) Failure Mechanism For Rectangular Footing

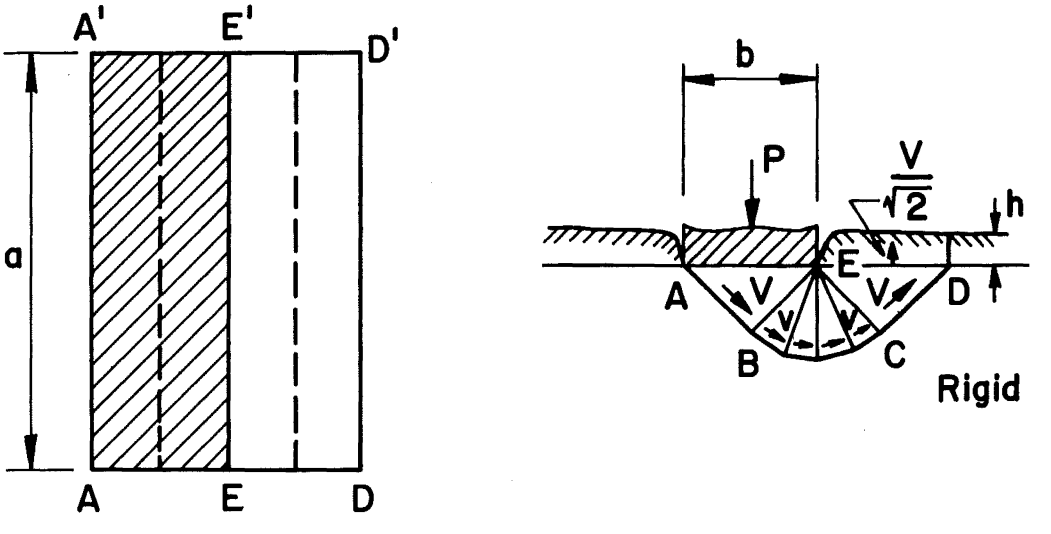

(b) Plan and Section In (a)

Fig. 26 Three-Dimensional Failure Mechanism for Bearing Capacity Porblem, $\emptyset=0$

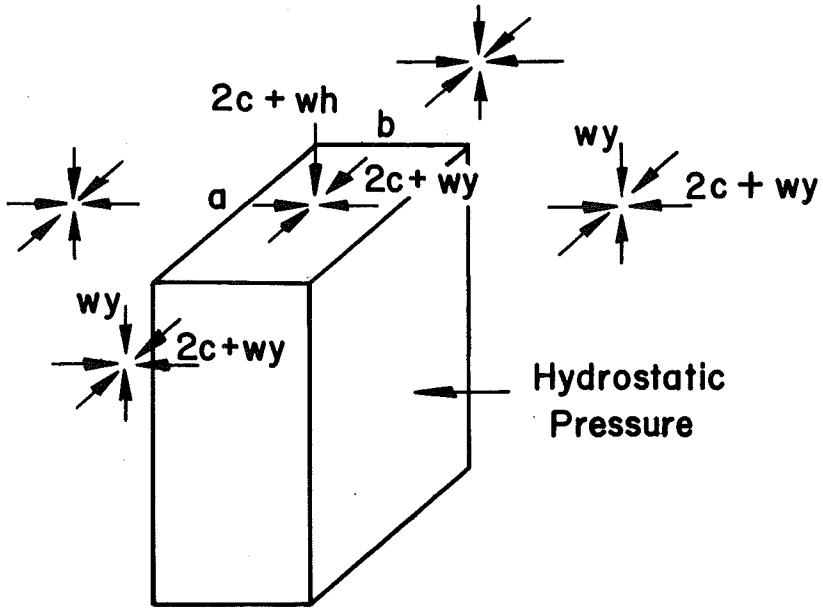

(a) Extension of Fig. 23 b

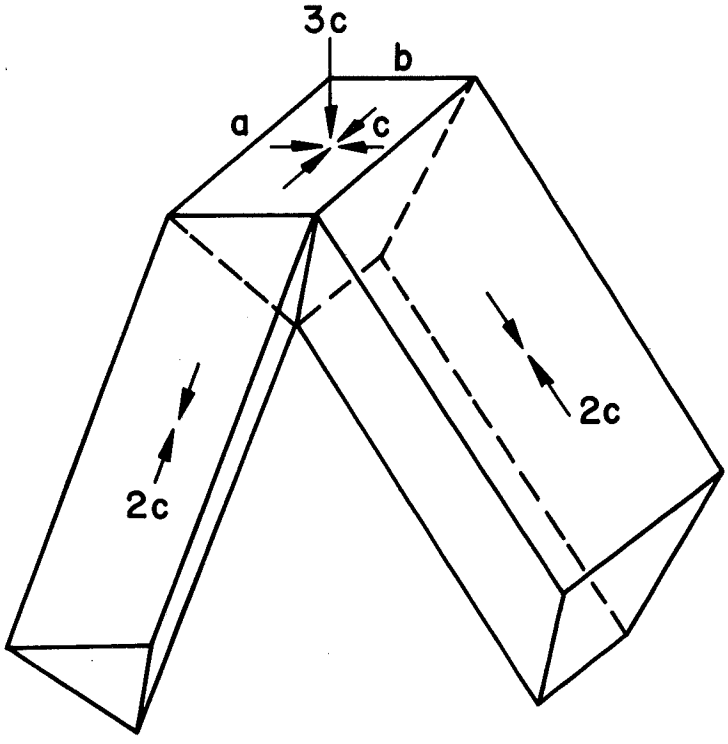

(b) Extension of Fig. 24 b

Fig. 27 Three-Dimensional Stress Field for Bearing Capacity Problem, $\emptyset=0$

9. APPENDIX

Energy dissipation in a log spiral zone of c-ϕ soils:

The extension of the discussion of energy dissipation to a zone of radial shear, which includes the more general case of a log spiral zone, for c-ϕ soils can also be developed. A slip δu must always be accompanied by a separation δv as discussed in Section 2. There is no need to consider the separation when the shear strength of a soil is due only to the cohesion. Consider the six rigid triangles at an equal angle $\Delta\theta$ to each other as shown in Fig. 8a and the corresponding compatible velocity diagram for two typical triangles A-O-B and B-O-C which are shown in Fig. 8b. If the central angle $\Delta\theta$ is sufficiently small, one may write:

$$\begin{aligned} V_1 &= V_o\,(1 + \Delta\theta\,\tan\phi) \\ V_2 &= V_1\,(1 + \Delta\theta\,\tan\phi) \\ &\vdots \\ V_n &= V_{n-1}\,(1 + \Delta\theta\,\tan\phi) \end{aligned} \tag{75}$$

The velocity in the nth triangle O-E-F is:

$$V_n = V_o\,(1 + \Delta\theta\,\tan\phi)^n \tag{76}$$

where V_o is the initial velocity. Clearly, the log spiral zone is obtained as a limiting case when the number of the rigid triangles grows to infinity. Hence, as $n \rightarrow \infty$, Eq. (76) becomes:

$$V_o\ (1 + \Delta\theta\ \tan\phi)^n = V_o\ (1 + \frac{\theta\tan\phi}{n})^n \rightarrow V_o\ \exp(\theta\tan\phi)$$

or (77)

$$V = V_o\ \exp(\theta\tan\phi)$$

where V is the velocity at any angular location, θ, along the spiral and which agrees with the value obtained by Shield[32].

From Equation (7), the rate of energy dissipation along a typical radial line, say O-B, is:

$$cr_2\ (V_1\Delta\theta) \tag{78}$$

where δu appears as $V_1\Delta\theta$. Similarly, the dissipation along the spiral surface A-B is:

$$c(\frac{r_2\Delta\theta}{\cos\phi})\ (V_1\ \cos\phi) \tag{79}$$

where the length of A-B is $(r_2\Delta\theta/\cos\phi)$ and $\delta u = V_1\ \cos\phi$. Again, the dissipation along a radial line is the same as along the spiral surface segment provided the central angle $\Delta\theta$ is small. Thus, the expression for energy dissipation in the log spiral zone will be identical with

the expression along the spiral surface which can be obtained by integrating Eq. (79) along the spiral surface $r=r_o \exp\theta\tan\phi$:

$$c \int rV \, d\theta = c \int_o^{\Theta} (r_o \, e^{\theta\tan\phi}) \, (V_o \, e^{\theta\tan\phi}) d\theta$$

$$= \frac{1}{2} c \, V_o \, r_o \cot\phi \, (e^{2\Theta\tan\phi} - 1) \qquad (80)$$

which agrees with the value obtained by Haythornthwaite[33].

10. NOMENCLATURE

b	punch width
c	cohesion
D	dissipation function
D_A	rate of dissipation of energy per unit area
F	force
H	height
k_a	coefficient of active earth pressure
k_p	coefficient of passive earth pressure
p	bearing capacity per unit area
P	load, force
r	radius
V	velocity
w	weight per unit volume
W	total weight
δv	discontinuous normal velocity
δu	discontinuous tangential velocity
$\alpha, \beta, \theta, \Omega$	angular parameter
$\dot{\alpha}, \omega$	angular velocity
$\dot{\gamma}$	engineering shear strain rate
$\dot{\gamma}_{max}$	maximum rate of engineering shear strain
δ	angle of wall friction
Δ	distance
$\dot{\epsilon}$	normal strain rate

$\dot{\epsilon}_t$	tensile principal component of the plastic strain rate tensor
σ	normal stress
τ	shear stress
ϕ	angle of internal friction
Θ	angular parameter defining zone of radial shear

11. REFERENCES

1. Terzaghi, K.
   THEORETICAL SOIL MECHANICS, New York, John Wiley and Sons, 1943.

2. Drucker, D. C.
   ON STRESS-STRAIN RELATIONS FOR SOILS AND LOAD CARRYING CAPACITY, Proceedings, First International Conference on the Mechanics of Soil-Vehicle Systems, Turin, Italy, Edicioni Minerva Technica, pp. 15-23, June 1961.

3. Sokoloviskii, V. V.
   STATICS OF GRANULAR MEDIA, First Edition, New York, Oxford, 1965.

4. Drucker, D. C.
   A MORE FUNDAMENTAL APPROACH TO STRESS-STRAIN RELATIONS, Proceedings of the First United States National Congress of Applied Mechanics, pp. 487-491, June 1951.

5. Drucker, D. C., Prager, W., Greenberg, H. J.
   EXTENDED LIMIT DESIGN THEOREMS OF CONTINUOUS MEDIA, Quarterly Applied Mathematics, Vol. 9, pp. 381-389, 1952.

6. Drucker, D. C., Prager, W.
   SOIL MECHANICS AND PLASTIC ANALYSIS OR LIMIT DESIGN, Quarterly Applied Mathematics, Vol. 10, pp. 157-165, 1952.

7. Drucker, D. C.
   LIMIT ANALYSIS OF TWO AND THREE DIMENSIONAL SOIL MECHANICS PROBLEMS, Journal of the Mechanics and Physics of Solids (Oxford), Vol. 1, No. 4, pp. 217-226, 1953.

8. Shield, R. T.
   ON COULOMB'S LAW OF FAILURE IN SOILS, Journal of the Mechanics and Physics of Solids, Vol. 4, No. 1, pp. 10-16, 1955.

9. Dais, J. L.
   AN ISOTROPIC FRICTIONAL THEORY FOR A GRANULAR MEDIUM WITH AND WITHOUT COHESION, Ph.D. Thesis, Applied Mathematics, Brown University, May 1967.

10. Brinch, Hansen J.
    EARTH PRESSURE CALCULATION, Danish Technical Press, 1953.

11. Drucker, D. C.
    COULOMB FRICTION, PLASTICITY, AND LIMIT LOADS, Journal of Applied Mechanics, Vol. 21, Transaction ASME, Vol. 76, pp. 71-74, 1965.

12. Drucker, D. C.
CONCEPTS OF PATH INDEPENDENCE AND MATERIAL STABILITY FOR SOILS, in "Rheologie et Mecanique Des Soils", Proceedings IUTAM Symposium, Grenoble, April 1964, Edited by J. Kra and P. M. Sirieys, Springer, pp. 23-43, 1966.

13. De Josselin De Jong, G.
LOWER BOUND COLLAPSE THEOREM AND LACK OF NORMALITY OF STRAIN-RATE TO YIELD SURFACE FOR SOILS, Rheology and Soil Mechanics, IUTAM Symposium, Grenoble, France, pp. 69-75, 1964.

14. Drucker, D. C., Gibson, R. E., Henkel, D. J.
SOIL MECHANICS AND WORK-HARDENING THEORIES OF PLASTICITY, Transaction ASCE, Vol. 122, pp. 338-346, 1957.

15. Jenike, A. W. and Shield, R. T.
ON THE PLASTIC FLOW OF COULOMB SOLIDS BEYOND ORIGINAL FAILURE, Journal of Applied Mechanics, Vol. 26, pp. 599-602, 1959.

16. Weidler, J. B. and Paslay
AN ANALYTICAL DESCRIPTION OF THE BEHAVIOR OF GRANULAR MEDIA, Engineering, Brown University Report 36, ARPA SD-86 November 1966.

17. Spencer, A. J. M.
A THEORY OF THE KINEMATICS OF IDEAL SOILS UNDER PLANE STRAIN CONDITIONS, Journal of Mechanics and Physics of Solids, Vol. 12, pp. 337-351, 1964.

18. Sobotka, Z.
NON-HOMOGENEITY IN ELASTICITY AND PLASTICITY, Proceedings IUTAM Symposium, Warsaw, Edited W. Olszak, Pergamon Press Limited, London, p. 227, 1958.

19. Sobotka, Z.
SOME AXIALLY SYMMETRICAL AND THREE-DIMENSIONAL PROBLEMS OF THE LIMIT STATES OF NON-HOMOGENEOUS CONTINUOUS MATTERS, Proceedings Tenth International Congress of Applied Mechanics, Stresa, Paper No. II-85, 1960.

20. Chen, W. F.
ON THE COULOMB YIELD SURFACE AND RATE OF DISSIPATION OF ENERGY, Fritz Engineering Laboratory Report No. 355.1, January 1968.

21. Chen, W. F.
ON SOLVING PLASTICITY PROBLEMS OF RELEVANCE TO SOIL MECHANICS, Engineering, Brown University Report, April 1968.

22. Fellenius, W.
ERDSTATISCHE BERECHNUNGEN, Berlin, W. Ernst und Sohn, 1927.

23. Kooharian, A.
LIMIT ANALYSIS OF VOUSSOIR (SEGMENTAL) AND CONCRETE ARCHES, Journal of American Concrete Institute, Vol. 24, pp. 317-328, 1952.

24. Chen, W. F. and Drucker, D. C.
THE BEARING CAPACITY OF CONCRETE BLOCKS OR ROCK, Engineering Mechanics Specialty Conference, Raleigh, North Carolina, November 1967.

25. Chen, W. F.
DISCUSSION ON APPLICATIONS OF LIMIT PLASTICITY IN SOIL MECHANICS, by W. D. Liam Finn, Journal of the Soil Mechanics and Foundations Division, Vol. 94, No. SM2, pp. 608-613, March 1968.

26. Coulomb, C. A.
ESSAI SUR UNE APPLICATION DES REGLES DES MAXIMIS ET MINIMIS A QUELQUES PROBLEMES DE STATIQUE RELATIFS A ARCHITECTURE, Mem. Acad, Roy, Pres. Sav. Etr., Vol. 7, 1776.

27. Finn, W. D. Liam
APPLICATIONS OF LIMIT PLASTICITY IN SOIL MECHANICS, Journal of the Soil Mechanics and Foundations Division, Vol. 93, No. SM5, pp. 101-119, September 1967.

28. Tschebotarioff, G. P.
SOIL MECHANICS, FOUNDATIONS, AND EARTH STRUCTURES, McGraw-Hill Book Company, New York, pp. 222-226, 1951.

29. Johnson, W. and Mellor, P. B.
PLASTICITY FOR MECHANICAL ENGINEERS, D. VanNostrand Company Incorporated, Princeton, New Jersey, pp. 295-296, 1962.

30. Drucker, D. C. and Chen, W. F.
ON THE USE OF SIMPLE DISCONTINUOUS FIELDS TO BOUND LIMIT LOADS, Brown University Report, March 1967, Engineering Plasticity, Edited by J. Heyman and F. A. Leckie, Cambridge University Press, 1968.

31. Shield, R. T. and Drucker, D. C.
THE APPLICATION OF LIMIT ANALYSIS TO PUNCH-INDENTATION PROBLEMS, Journal of Applied Mechanics, ASME, Vol. 75, pp. 453-391, 1951.

32. Shield, R. T.
MIXED BOUNDARY VALUE PROBLEMS IN SOIL MECHANICS, Quarterly Applied Mathematics, Vol. 11, No. 1, pp. 61-76, 1954.

33. Haythornthwaite, R. M.
METHODS OF PLASTICITY IN LAND LOCOMOTION STUDIES, Proceedings, First International Conference on the Mechanics of Soil Vehicle Systems, Turin, pp. 3-19, 1961.